Extreme cold will still occur in Northern Europe, although less often - risking decreasing preparedness and higher vulnerability

Authors

1. Izidine Pinto, *Royal Netherlands Meteorological Institute (KNMI), De Bilt, The Netherlands*
2. Mika Rantanen,*Finnish Meteorological Institute, Helsinki, Finland*
3. Karianne Ødemark, *Norwegian Meteorological Institute, Oslo, Norway*
4. Jordis Tradowsky, *Norwegian Meteorological Institute, Oslo, Norway*
5. Erik Kjellström, *Rossby Centre, Swedish Meteorological and Hydrological Institute (SMHI), Norrköping, Sweden*
6. Clair Barnes*, Grantham Institute, Imperial College London, UK*
7. Friederike E L Otto, *Grantham Institute, Imperial College London, UK*
8. Dorothy Heinrich, *Red Cross Red Crescent Climate Centre, The Hague, the Netherlands*
9. Carolina Pereira Marghidan, *Red Cross Red Crescent Climate Centre, The Hague, the Netherlands; Royal Netherlands Meteorological Institute (KNMI), De Bilt, The Netherlands; Faculty of Geo-Information Science and Earth Observation (ITC), University of Twente, Enschede, the Netherlands*
10. Maja Vahlberg, *Red Cross Red Crescent Climate Centre, The Hague, the Netherlands*
11. Knud Falk, *Red Cross Red Crescent Climate Centre, The Hague, the Netherlands*
12. Robert Vautard, *Institut Pierre-Simon Laplace, CNRS, Sorbonne Université, Paris, France*
13. Sarah Kew, *Royal Netherlands Meteorological Institute (KNMI), De Bilt, The Netherlands*
14. Sjoukje Philip, *Royal Netherlands Meteorological Institute (KNMI), De Bilt, The Netherlands*

Review authors

1. Joyce Kimutai, *Grantham Institute, Imperial College London, UK*
2. Mariam Zachariah, *Grantham Institute, Imperial College London, UK*
3. Julie Arrighi, *Red Cross Red Crescent Climate Centre, The Hague, the Netherlands*
4. Anders Forsberg, *Swedish Red Cross, Stockholm, Sweden*
5. Niklas Vaalgamaa, *Finnish Red Cross*
6. Lotta Scheider, *Swedish Red Cross, Stockholm, Sweden*

Main findings

- Extreme cold such as experienced during this event can have severe direct impacts on health, and secondary impacts on roads, electricity grids, and services such as schools and public transport.
- Cold waves, like other extreme weather events, put significant pressure on energy, healthcare, and water systems. These systems must be designed and able to absorb additional (or different) needs, and early warnings, preparedness plans, and response capacity are all crucial to mitigate the impacts of these events.
- Homelessness in particular, but also energy poverty and bottlenecks with the associated price hikes and, in some cases, poor housing conditions, exacerbate the impacts of cold waves on particularly vulnerable socio-economic and demographic groups.

- Even though some very low temperatures were recorded, the dataset based on observations characterises the area average 5-day cold spell as a 1-in-15 year event in today's climate, ranking as 12th coldest since 1950. For Oslo, the one day minimum temperature was rare, approximately a 1-in-200 year event in today's climate.
- To estimate the influence of human-caused climate change on this extreme cold we use a combination of climate models and the observations. We find that because of human-induced climate change the area-averaged event would have been about 4 degrees colder in a 1.2°C cooler climate. This corresponds to such cold spells having become about 5 times less frequent.
- For the Oslo station the cold single day minimum would also have been about 4 degrees colder without human-induced climate change. This corresponds to such cold days having become about 12 times less frequent.
- At global mean temperatures of 2°C above pre-industrial levels, large-scale cold spells as rare as this one are projected to be about another 2.5 °C less cold for the area average and about another 2 °C less cold for Oslo. They will become even less frequent than today.
- Climate change does not mean that cold waves will no longer happen. In fact, less severe and less frequent cold waves may be more impactful than past ones if risk perception and preparedness decrease due to the less frequent event occurrences.

1 Introduction

In January 2023, Norway, Sweden and Finland (together referred to as Fennoscandia) experienced an intense cold wave event. On 5 January -44.3°C was recorded at Enontekiö airport in Finland and Vittangi in Sweden reported -44.6°C, the lowest temperatures recorded in Fennoscandia in the 21st century. At Blindern Oslo, the minimum daily temperature during the night of the 6th of January reached -23.1°C, which is the lowest temperature registered at this station since 1987. Notably, this extreme level of cold temperature has been surpassed only 15 times in the observation records that go back to 1937. The last cold event occurred on January 1st of 1979. In Sweden, the centennial station Abisko recorded its lowest temperature of -35.2°C on January 4th, marking the 11th lowest annual temperature on record starting in 1913.

While Fennoscandia is generally well-equipped and accustomed to winter conditions, the region has experienced a decrease in very cold temperatures in recent times. The temperatures that were felt in some places over the region during the first week of January were significant reminders of the risks posed by extreme cold, particularly for certain vulnerable groups and systems. However, daily life and livelihoods of people were severely interrupted by the cold wave notably through transport services and the closure of roads. The extreme weather caused traffic disruptions, school closures and a high number of insurance claims, mainly due to frozen pipes (NewsInEnglish, 2023). In addition to the cold temperatures, high volumes of snowfall lead to issues specifically in the southern part of the country that experiences less snow than the Arctic north of Norway in general.

The record temperatures that were felt in some places over the region during the first week of January were significant reminders of the risks posed by extreme cold, particularly for certain vulnerable groups and systems, and daily life and livelihoods of people were significantly interrupted for the few days of the cold waves.

In Sweden and Finland, the cold spell led to disruptions in transportation services, with train cancellations attributed to frozen brakes and concerns about passenger safety in the event of unplanned stops. The surge in electricity prices was notable due to both high demand and low production caused by minimal wind. In Southern Sweden, approximately 1,000 cars and trucks were trapped overnight in a snowstorm and rescue services and the army worked to free passengers on Thursday morning (the Guardian 2024, BBC, 2024); voluntary services along the road provided assistance to many of the affected people and sports arenas opened for temporary shelter (Dagens Nyheter 2024). In Finland, electricity prices hit a record high on Friday 5 January due to strong demand caused by cold weather, but simultaneous failures at the power plants also reduced the supply of electricity (Yle, 2024). Instances of broken water pipes in homes resulted in leaks and water damage, both presently and anticipated in the upcoming spring. Additionally, the event heightened demand for rescue services as people increased their use of fireplaces for heating, leading to more fires.

The cold was not entirely unexpected. On January 3, an outbreak of cold polar air led to extreme cold weather conditions in Sweden, Finland and Norway, and on January 8, it brought about the first frost of the year in the Netherlands (KNMI,2023). A development of an anticyclone over northern Scandinavia, allowed very cold Arctic air masses to flow from the northeast towards northern Europe. Although the lower tropospheric air mass in northernmost Scandinavia was not anomalously cold, the low winds in the vicinity of the anticyclone, cloudless skies and extensive snow cover allowed a strong inversion layer to form near the surface. The stable surface layer prevented mixing with the upper air layers, and continuous radiative cooling in the twilight of the polar night allowed temperatures to fall below -40°C at several weather stations. The coldest air masses subsequently moved towards southern Scandinavia. As wind speeds dropped, -31.1°C was recorded on 6 January in Bjørnholt, Oslo, which was the coldest temperature ever recorded in the area. However, it is important to note here that this occurred in a rural area of low population density and would not have been experienced by many people; the minimum temperature in Oslo Blindern in the city was -23.1°C, where the record of -26°C from 1942 remains unbroken. Air masses arriving over Northern Scandinavia on the coldest days originated from Northern Russia and polar ice-covered regions five days earlier, where in this time of year sunlight is absent or very weak, and thereby no chance to warm. This air mass has been descending from the mid-troposphere (under adiabatic warming contributing to the stable conditions and ultimately the strong inversion close to ground) without contact to the cold ice-covered polar ocean. (see Figure A1).

The cold event started in the north and moved south. Therefore, to cover the impacts of the cold in Fennoscandia, we use area-averaged daily minimum temperatures (Tmin) over the most affected region to define the event for the attribution study. The selected study area covers the region 62°N-70°N, 10°E-30°W and is outlined in Figure 1. Defining the year to run from July to June, we choose the annual (Jul-Jun) minimum of an average over 5-days (TN5day) to capture the temporal scale of the event. The study domain recorded the coldest 5-day daily mean averaged minimum temperatures over the region in the month of January.
Additionally we analyse station data at three different stations: The Swedish Abisko station that is within the box defined above, the Finnish station of Helsinki just south of the box, and the Norwegian station Blindern in Oslo. For the station locations we use a temporal event definition of annual

(Jul-Jun) minima of 1-day minimum temperatures, TN1day. Lastly, to cover the impacts of the cold wave in the Oslo area, we also do an attribution analysis for the Oslo station.

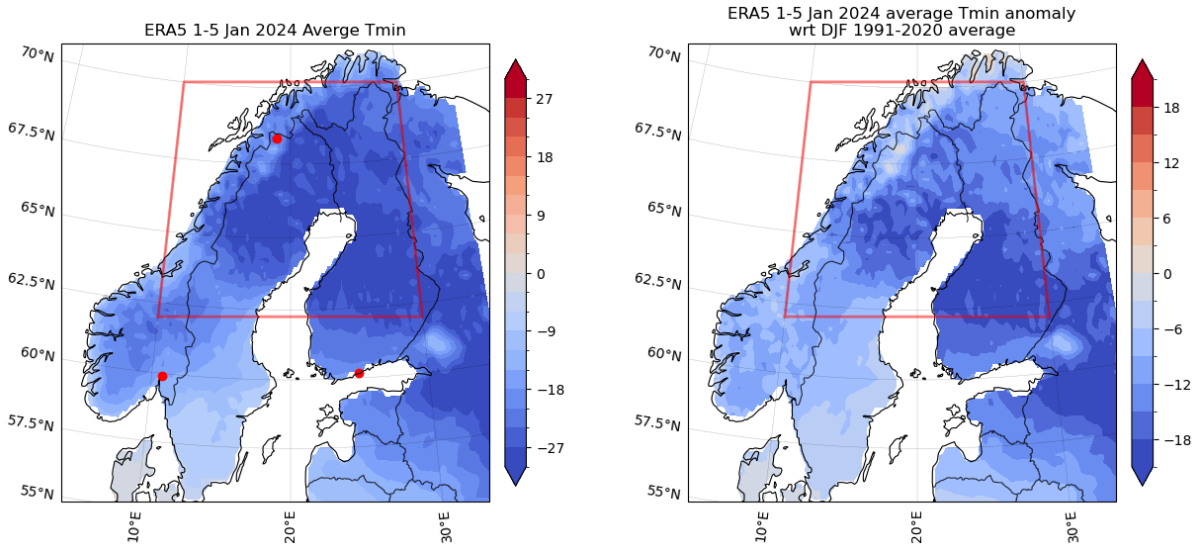

Figure 1. *ERA5 near surface minimum temperature (Tmin) [°C] showing 5-day average of daily minimum temperature for the period of 1st to 5th January 2024 (left) and anomalies wrt the 1991-2020 DJF averaged minimum temperatures (right). The red outline represents the study region [62°N-70°N, 10°E-30°W]. The dots mark stations used in the observational analysis: Oslo in Norway, Helsinki in Finland and Abisko in Sweden.*

In general, cold waves in the northern midlatitudes are becoming milder (van Oldenborgh et al. 2019 ; Cattiaux et al., 2010). One reason for this is the strong warming trend in the source region of cold air masses, i.e. in the Arctic, driven by anthropogenic warming of the climate system (Arctic Amplification). For example, in northern Europe, cold-season temperatures associated with the northerly flow from the Arctic (i.e. negative North Atlantic Oscillation, NAO) have warmed about 60% faster than those weather patterns where air flows from the North Atlantic (NAO+) (Rantanen et al. 2023).

These findings are in line with global assessments, showing a stronger increase in minimum temperatures compared to maximum temperatures. The IPCC assessed the warming of cold extremes in Arctic regions to be three times higher than the global average. This more rapid increase in temperatures of cold extremes in the Arctic regions is projected to continue with a factor of 3 with future global warming. The snow/ice albedo effect plays an important role in this rapid warming of cold extremes in high latitudes in the Northern Hemisphere (Seneviratne et al., 2021).

2 Data and methods

2.1 Observational data

Daily minimum temperature observations for three stations (Fig. 1a, Figs. 3a-5a) over Sweden, Norway and Finland were made available by the national meteorological and hydrological institutes of the respective countries. Abisko is located at 392.3 m above sea level (a.s.l.) in the mountains in the

far north of Sweden (68.36N, 18.82E). Data is available from 1913 to 10 January 2024. Oslo Blindern is located 94m a.s.l. (59.95° N 10.72° E). Data is available from 1937 to 11 January 2024. The station has been at the same location for the whole measuring period. The surroundings close to the station have remained unchanged, although there are some more buildings in the area today compared to when the observation series started. Helsinki Kaisaniemi, is located in a park within the city centre (60.16°N, 24.93°E) with an elevation of four metres above sea level. The weather station has been located in Kaisaniemi for its entire history since 1844, although in 1962 it was moved a few hundred metres to its current site in the University Botanic Garden. The impact of urbanisation in the city of Helsinki on temperature was greatest in the 19th century and the early decades of the 20th century. Daily temperatures from Helsinki Kaisaniemi do not take urbanisation into account, but the monthly averages are corrected for urbanisation.

In addition to stations, we use daily minimum temperatures (Tmin) from the European Centre for Medium-Range Weather Forecasts (ECMWF) ERA5 reanalysis product (Hersbach et al., 2020). It should be noted that the variables from ERA5 are not direct observations, but instead are generated by atmospheric components of the Integrated Forecast System (IFS) that assimilates the observations. The reanalysis begins in 1950, with data available until the end of December 2023. We extend the reanalysis data with the preliminary ECMWF analysis (1-7 January 2024) to cover the period of the event. While this is preliminary data, it is unlikely to affect the main conclusions of the analysis.
As a measure of anthropogenic climate change we use the (low-pass filtered) global mean surface temperature (GMST) taken from the National Aeronautics and Space Administration (NASA) Goddard Institute for Space Science (GISS) surface temperature analysis (GISTEMP, Hansen et al., 2010 and Lenssen et al. 2019).

2.2 Model and experiment descriptions

We use two multi-model ensembles from climate modelling experiments using different framings (Philip et al., 2020): Regional climate models and coupled global circulation models and regional climate models.

1. Coordinated Regional Climate Downscaling Experiment (CORDEX)- European Domain (EURO-CORDEX) with 0.11° resolution (Jacob et al., 2014; Vautard et al., 2021). The ensemble consists of 50 runs from a combination of 11 regional climate models (RCMs) with boundary conditions from eight GCMs. These simulations are composed of historical simulations from 1950 or 1970 up to 2005, and extended to the year 2100 using the RCP8.5 scenario.

2. CMIP6. This consists of simulations from 19 participating models with varying resolutions. For more details on CMIP6, please see Eyring et al., (2016). For all simulations, the period 1850 to 2015 is based on historical simulations, while the SSP5-8.5 scenario is used for the remainder of the 21st century.

2.3 Statistical methods

In this study, we analyse time series from the area average over the box 62°N-70°N; 10°E-30°E of ERA5 Tmin (see Fig. 1) as well as Tmin time series of the stations Oslo Blindern, Helsinki and Abisko (see Figs. 3-5). Methods for observational and model analysis and for model evaluation and

synthesis are used according to the World Weather Attribution Protocol, described in Philip et al. (2020), with supporting details found in van Oldenborgh et al. (2021), Ciavarella et al. (2021).

The analysis steps include: (i) trend calculation from observations; (ii) model evaluation; (iii) multi-method multi-model attribution and (iv) synthesis of the attribution statement.
We calculate the return periods, Probability Ratio (PR; the factor-change in the event's probability) and change in intensity of the event under study in order to compare the climate of now and the climate of the past, defined respectively by the GMST values of now and of the preindustrial past (1850-1900, based on the Global Warming Index). To statistically model the event being analysed, we use a Generalised Extreme Value (GEV) distribution that shifts with GMST for the TN5day (study region average from ERA5 gridded dataset) and TN1day (station data). Next, for the region average. results from observations and models that pass the evaluation tests are synthesised into single attribution statements.

3 Observational analysis: return period and trend

3.1 Analysis of point station data and gridded data

Using ERA5 reanalysis data, we analyse the area average (red box from Figure 1a) for TN5day. We calculate the return period, change in intensity and probability ratio (with 95% confidence intervals) between 2023/2024 and a past climate that is 1.2°C cooler than now through fitting a GEV model. The annual minimum time series and the fit to the GEV model are shown in Figure 2. The interannual variability of TN5day shows a clear increasing trend, suggesting that these events are becoming warmer. The 2023/24 event of the TN5day with a value of -25.006 ℃ occurs over 1-5 January 2024. The return period over the area average for this event is 15.7 years (7.45 to 147 years). For the model analysis we use a rounded value of 15 years. The change in intensity is 4.254 ℃ (1.680 ℃ to 6.667 ℃) between the past and present climate. The probability ratio is 0.191 (0.023 to 0.575) between the past (1.2 ℃ cooler) and present climate. Note that a probability ratio < 1 means that this type of event nowadays happens *less* often than in the past, 1.2 ℃ cooler climate. Taking the inverse shows us that an event of this magnitude occurs 5.22 (1.74 to 43.2) times less often now, as compared to the pre-industrial past.

We tested the sensitivity of this event definition by using a region that is the same over Norway and Sweden, but extending further south over Finland to include the Helsinki station. The results were very similar to the results using the original area.

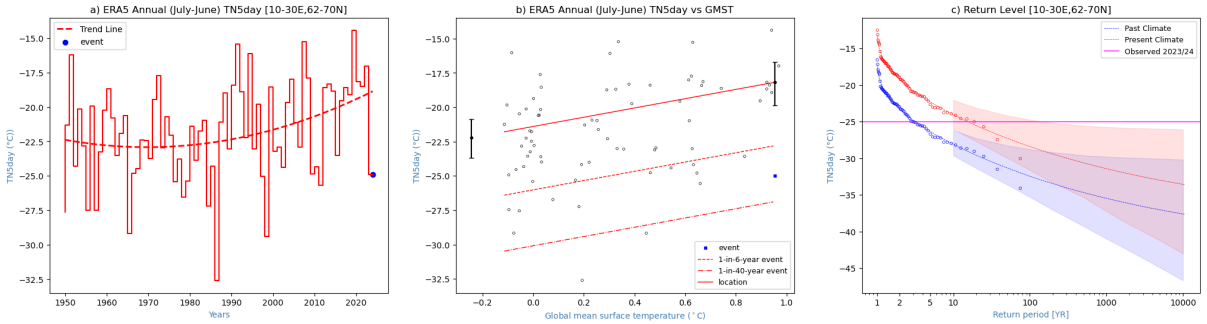

Figure 2. Annual minimum of TN5day over the study region shown in Figure 1. The dotted red line represents the quadratic fit and the blue dot shows the event TN5day=-25°C (a), TN5day data over the study region estimated from ERA5 records shown against the change in global mean temperature. The thick red line denotes the time-varying mean. The vertical black lines show the 95% confidence interval for the location parameter, for the current, 2023/24 climate and the hypothetical, 1.2ºC cooler climate. The 2024 observation is highlighted with the blue box (b). Return periods for the 2023/24 climate (red lines) and the 1.2ºC cooler climate (blue lines with 95% CI), based on ERA5 data (1950/51-2023.ext-2024).

Next, we repeat the analysis using station data, for the four selected stations - Oslo Blindern, Abisko and Helsinki, but for TN1day to estimate the return period, intensity change and probability ratio. The annual minimum time series and the fits to the GEV model are shown in Figs. 3-5.

For Oslo Blindern there has been an overall trend towards less cold extremes (Fig 3a). The event TN1day value at this weather station is -23.1 ℃. The return period for such a temperature at this station is 237 years (at least 38.6 years) in the 2023/24 climate. For the model analysis we use a rounded value of 200 years. The change in intensity is 5.032 ℃ (2.478 ℃ to 8.090 °C) between the past and present climate. The uncertainty around the probability ratio is too large to attach a meaningful value to it (see Table 4). Results for TN5day are, except for the smaller return period, not much different: the return period of is 42.393 years (15.19 to 2134 years) and the change in intensity 4.554 ℃ (1.958 ℃ to 7.220℃) between the past and present climate. The annual temperature for Norway as a whole has increased by approximately 1.3 degrees from 1900 to 2023 based on the annual report for 2023 issued by the Norwegian Meteorological Institute (data can be found at seklima.met.no). The largest increase in temperatures occurred over the last two decades with most years being anomalously warm. The annual mean temperature in Oslo has increased by 1.5 °C in the period 1838–2012 (Nordli et al, 2015). The temperature has increased significantly in all seasons; however, the temperature increase in winter and spring is more than double the increase in summer. The recent report by Gjelten et al (2023) indicated that the minimum and maximum temperatures in Oslo experienced a continued increase by 2020.

For Abisko the event TN1day value is -35.2℃. The return period for this station is 27.8 years (11.6 to 12066 years) in the 2023/24 climate. The change in intensity is 1.985 ℃ (0.116 ℃ to 4.035 ℃) between the past and present climate. The probability ratio is 0.299 (0.025 to 1.40), which again means that an event with such magnitude happens less often nowadays than in the past (1.2 ℃ cooler climate), although the change is not significant as it encompasses 1. Once again, the results for TN5day are not much different: the return period of the event is higher, with 31.1 years (10.7 to 255 11 years), and the trend only slightly smaller, although it encompasses the possibility of no change: the change in intensity is 1.693 ℃ (-0.568 ℃ to 3.843 ℃) and the probability ratio is 0.312 (0.033 to 1.575). Finally, we also checked the sensitivity of both definitions - TN1day and TN5day to the length of the time series. If we only use data from 1950 onwards (similar to ERA5) rather than from 1912 onwards, the trend becomes larger. Starting in 1950, for TN1day the return period is 56.4 years (at least 17.2 years) and the change in intensity is 3.558 ℃ (0.830 ℃ to 6.455 ℃). The probability ratio is then 0.094 (at least 0.002). This corroborates the evidence that accelerated warming has been experienced since 1950 (IPCC, 2021). Results for TN5N starting in 1950 are similar to those of TN1day starting in 1950. Since the end of the 19th century, temperatures in Sweden have increased in

all seasons with the largest increases in winter (DJF) and spring (MAM) as described in Schimanke et al. (2022). The observations also show a prevalence for record low temperatures in the earlier part of the records while record high temperatures are more common in the last decades. In a study linking temperature anomalies to large-scale circulation, Kjellström et al. (2022) show that Swedish temperatures have increased in most circulation types for all months comparing 1991-2020 with 1961-1990 based on ERA5 data. They also found decreasing temperature variability during winter.

For Helsinki, there has been a trend toward decreases in cold events. The magnitude of the 2024 event measured as TN1day is -21.2 ℃. The return period for this station is 3.6 years (2.2 to 7.1 years) in the current climate. The change in intensity is 4.764 ℃ (2.125 ℃ to 7.349 ℃). The probability ratio is 0.393 (0.189 to 0.676), which again means such a cold wave happens less often nowadays than in a 1.2 ℃ cooler climate. Results for a 5-day average are not much different, consistent with the nature of results reported for the other stations: the return period of TN5day is 5.2 years (3.0 to 11 years), the change in intensity 4.5767 ℃ (2.162 ℃ to 7.331 ℃) and the probability ratio is 0.329 (0.142 to 0.617).

As the station data run over longer times - going back as far as 1844, we checked the sensitivity of results to the length of the time series and possible inhomogeneities at the beginning of the series, by comparing them against the numbers from using data from 1880 and 1950 onwards (consistent with ERA5). The differences (higher trends and lower return periods if we use data from 1950) are ascribed to the behaviour of data prior to 1950 at the stations. Notwithstanding these differences, the overall increase in trends suggest that TN1day and TN5day events tend to be less colder now as compared to the pre-industrial past.

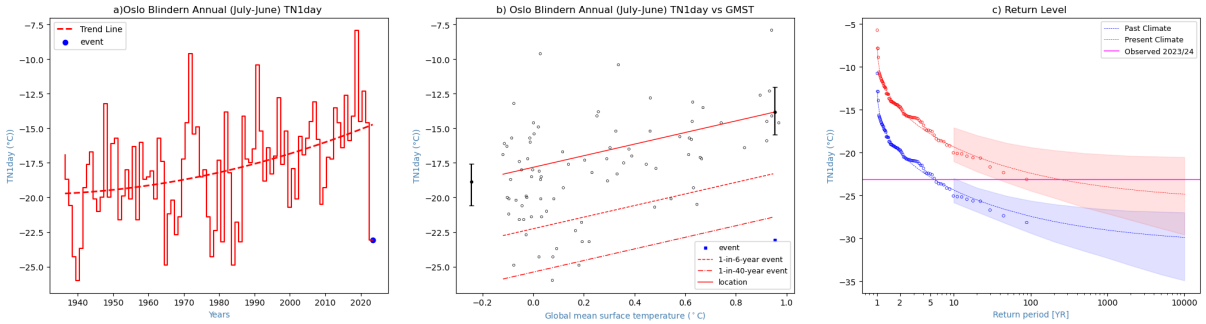

Figure 3. Same as Figure 2 but for TN1day for Oslo Blindern station (1936/37-2023-24)

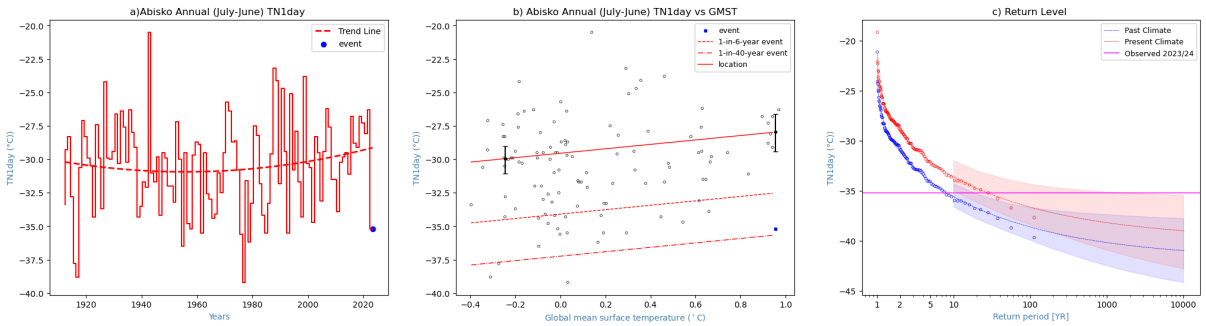

Figure 4. Same as Figure 2 but for TN1day for Abisko station (1912/13-2023/24)

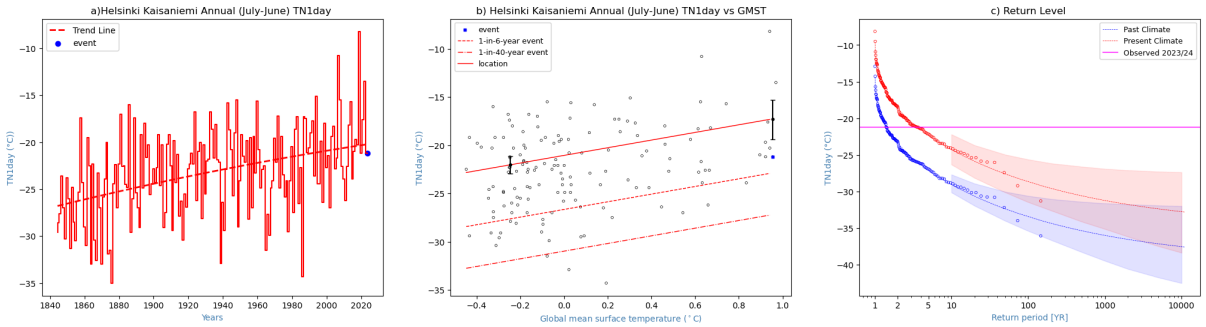

Figure 5. Same as Figure 2 but for TN1day for Helsinki Kaisaniemi station (1878/79-2023/24 - fitting period)

4 Model evaluation

In the subsections below we show the results of the model evaluation for the area average and the Oslo station area. As for both event definitions we have five or more models for CMIP6 and for CORDEX that pass the evaluation tests with the overall label 'good' we only use the models that perform well. We labelled models with 'bad' if two of the tests resulted in label 'reasonable' or if the fit parameters ranges hardly overlap (see point 3. below). We exclude all 'bad' models. In addition, models for which the return period differs from observations by 5°C (T>5) or more are excluded. Table 1 shows the model evaluation results. The climate models are evaluated against the observations in their ability to capture:

1. Seasonal cycles: For this, we qualitatively compare the model outputs against observations-based plots. We discard the models that exhibit multi-modality and/or ill-defined peaks in their seasonal cycles. We also discard the model if temperature seasonality varies significantly from the observations (Figures A3-4, A6-11) .

2. Spatial patterns: Models that do not match the observations in terms of the spatial patterns are excluded (Figures A2, A5).

3. Parameters of the fitted GEV model. We discard the model if the model and observation parameters ranges do not overlap (Tables 1,2).

4.1 Area average

For both the CMIP6 and the CORDEX ensemble there were more than 5 models with the label 'good', so we only use the models that perform well.

Table 1. Evaluation results of the climate models considered for attribution analysis of Tmin over the area average. For each model, the expected temperature of a 1-in-15 -year event is shown, along with the best estimate of the Sigma and Shape parameters and a 95% confidence interval for each, obtained via bootstrapping. The qualitative evaluation is shown in the right-hand column. Based on overall suitability, the models are classified as good, reasonable or bad, shown by green, yellow and red highlights, respectively.

Model / Observations	Seasonal cycle	Spatial pattern	Sigma	Shape parameter	Event magnitude [°C]	Conclusion
ERA5 box			-3.10 (-3.57 ... -2.53)	-0.16 (-0.40 ... -0.018)	-25.006	
CMIP6 GCMs					**Threshold for return period 15yr event**	
ACCESS-CM2	good	good	-2.69 (-3.15 ... -2.19)	-0.20 (-0.48 ... -0.060)	-27.9	good
ACCESS-ESM1-5	good	good	-2.61 (-3.12 ... -1.96)	-0.31 (-0.69 ... -0.17)	-19.76	bad, T>5
CanESM5	good	good	-2.86 (-3.35 ... -2.31)	-0.16 (-0.55 ... 0.030)	-24.37	good
CMCC-ESM2	good	good	-3.36 (-4.11 ... -2.50)	0.0 (-0.23 ... 0.26)	-29.36	reasonable
CNRM-CM6-1-HR	good	good	-2.57 (-2.95 ... -2.00)	-0.23 (-0.42 ... -0.10)	-25.09	good
CNRM-CM6-1	good	good	-2.79 (-3.37 ... -2.13)	0.010 (-0.23 ... 0.27)	-26.74	reasonable
EC-Earth3	good	good	-3.31 (-3.89 ... -2.59)	-0.25 (-0.43 ... -0.070)	-26.36	good
EC-Earth3-Veg	good	good	-3.20 (-3.77 ... -2.49)	-0.32 (-0.60 ... -0.16)	-25.48	good
EC-Earth3-Veg-LR	good	good	-4.17 (-5.26 ... -3.22)	-0.44 (-0.76 ... -0.20)	-28.21	reasonable
FGOALS-g3	bad	bad	-3.42 (-3.92 ... -2.82)	-0.36 (-0.57 ... -0.19)	-41.05	bad, spatial pattern&seasonal cycle & T>5
INM-CM4-8	good	good	-3.24 (-3.81 ... -2.44)	-0.29 (-0.54 ... -0.090)	-31.3	bad, T>5
INM-CM5-0	good	good	-3.40 (-3.99 ... -2.63)	-0.30 (-0.45 ... -0.15)	-29.87	good
IPSL-CM6A-LR	good	good	-3.92 (-4.63 ... -3.07)	-0.23 (-0.47 ... 0.020)	-31.66	bad, T>5
MIROC6	good	good	-2.85 (-3.30 ... -2.20)	-0.18 (-0.40 ... 0.020)	-24.34	good
MPI-ESM1-2-HR	good	good	-3.12 (-3.64 ... -2.49)	-0.26 (-0.55 ... -0.14)	-28.59	good
MPI-ESM1-2-LR	good	good	-2.83 (-3.48 ... -2.19)	-0.30 (-0.58 ... -0.070)	-24.64	good
MRI-ESM2-0	good	good	-3.08 (-3.61 ... -2.43)	-0.15 (-0.34 ... 0.030)	-19.71	bad, T>5
NorESM2-LM	good	good	-3.29 (-3.81 ... -2.77)	-0.18 (-0.40 ... -0.030)	-24.39	good
NorESM2-MM	good	good	-3.23 (-3.73 ... -2.70)	-0.19 (-0.36 ... -0.020)	-26.93	good
CORDEX RCMs						
CanESM2_CLMcom-CCLM4-8-17	good	good	-3.47 (-3.98 ... -2.82)	-0.31 (-0.48 ... -0.14)	-23.56	good
CanESM2_GERICS-REMO2015	good	good	-3.36 (-3.92 ... -2.52)	-0.25 (-0.57 ... -0.030)	-26.68	good
CNRM-CM5_CLMcom-CCLM4-8-17	good	good	-1.97 (-2.43 ... -1.36)	-0.060 (-0.24 ... 0.28)	-23.26	bad
CNRM-CM5_CLMcom-ETH-COSMO-crCLIM-v1-1	good	good	-2.43 (-2.83 ... -1.83)	-0.23 (-0.49 ... -0.080)	-21.75	reasonable
CNRM-CM5_SMHI-RCA4	good	good	-3.32 (-4.72 ... -2.26)	-0.46 (-1.1 ... -0.090)	-30.1	bad, T>5
EC-EARTH_CLMcom-CCLM4-8-17	good	good	-3.02 (-3.93 ... -2.12)	-0.29 (-0.81 ... 0.050)	-21.52	good

EC-EARTH_CLMcom-ETH-COSMO-crCLIM-v1-1	good	good	-2.49 (-2.90 ... -1.90)	-0.21 (-0.54 ... -0.050)	-18.76	bad, T<5
EC-EARTH_DMI-HIRHAM5	good	good	-2.75 (-3.21 ... -2.15)	-0.12 (-0.34 ... 0.080)	-21.41	good
EC-EARTH_GERICS-REMO2015	good	good	-3.88 (-4.63 ... -2.90)	-0.25 (-0.55 ... 0.010)	-25.55	reasonable
EC-EARTH_ICTP-RegCM4-6	good	good	-2.90 (-3.76 ... -2.14)	-0.34 (-1.0 ... -0.060)	-23.29	good
EC-EARTH_IPSL-WRF381P	good	good	-3.12 (-3.64 ... -2.45)	-0.31 (-0.60 ... -0.14)	-21.32	good
EC-EARTH_KNMI-RACMO22E	good	good	-2.60 (-3.12 ... -2.02)	-0.23 (-0.52 ... -0.040)	-21.64	good
EC-EARTH_MOHC-HadREM3-GA7-05	good	good	-3.41 (-3.94 ... -2.74)	-0.16 (-0.46 ... 0.030)	-28.21	good
EC-EARTH_SMHI-RCA4	good	good	-3.02 (-3.82 ... -2.20)	-0.23 (-0.68 ... -0.030)	-25.64	good
EC-EARTH_UHOH-WRF361H	good	good	-4.22 (-5.32 ... -3.28)	-0.17 (-1.1 ... 0.040)	-26.95	reasonable
IPSL-CM5A-LR_DMI-HIRHAM5	good	good	-3.11 (-3.56 ... -2.58)	-0.38 (-0.60 ... -0.25)	-28.13	good
IPSL-CM5A-LR_GERICS-REMO2015	good	good	-2.52 (-3.12 ... -1.97)	-0.31 (-0.76 ... -0.18)	-29.55	good
IPSL-CM5A-LR_IPSL-WRF381P	good	good	-2.76 (-3.37 ... -2.23)	-0.32 (-0.75 ... -0.10)	-27.91	good
IPSL-CM5A-LR_KNMI-RACMO22E	good	good	-3.25 (-3.76 ... -2.67)	-0.41 (-0.60 ... -0.25)	-27.17	reasonable
IPSL-CM5A-LR_SMHI-RCA4	good	good	-2.95 (-3.26 ... -2.32)	-0.56 (-0.50 ... -0.50)	-29.16	bad
MIROC5_CLMcom-CCLM4-8-17	good	good	-2.24 (-2.62 ... -1.79)	-0.17 (-0.53 ... -0.030)	-22.62	reasonable
MIROC5_GERICS-REMO2015	good	good	-3.21 (-3.99 ... -2.32)	-0.28 (-0.59 ... 0.0)	-29.07	good
HadGEM2-ES_CLMcom-CCLM4-8-17	good	good	-2.64 (-3.16 ... -2.04)	-0.15 (-0.32 ... 0.010)	-21.46	good
HadGEM2-ES_CLMcom-ETH-COSMO-crCLIM-v1-	good	good	-2.72 (-3.17 ... -2.14)	-0.20 (-0.42 ... -0.050)	-20.25	good
HadGEM2-ES_CNRM-ALADIN63	good	good	-2.21 (-2.59 ... -1.77)	-0.34 (-0.56 ... -0.17)	-20.66	reasonable
HadGEM2-ES_GERICS-REMO2015	good	good	-3.80 (-4.50 ... -3.06)	-0.27 (-0.56 ... -0.14)	-25.7	reasonable
HadGEM2-ES_ICTP-RegCM4-6	good	good	-5.05 (-7.03 ... -2.53)	-0.56 (-1.0 ... -0.060)	-28.56	bad
HadGEM2-ES_IPSL-WRF381P	good	good	-2.59 (-3.07 ... -1.92)	-0.19 (-0.43 ... -0.040)	-21.1	good
HadGEM2-ES_MOHC-HadREM3-GA7-05	good	good	-3.34 (-3.88 ... -2.68)	-0.20 (-0.46 ... -0.050)	-27.5	good
HadGEM2-ES_SMHI-RCA4	good	good	-4.20 (-5.05 ... -3.15)	-0.23 (-0.64 ... -0.04)	-25.25	good
HadGEM2-ES_UHOH-WRF361H	good	good	-4.36 (-5.35 ... -2.93)	-0.26 (-0.47 ... 0.0)	-26.45	reasonable
MPI-ESM-LR_CLMcom-CCLM4-8-17	good	good	-3.14 (-4.03 ... -2.36)	-0.16 (-0.65 ... 0.14)	-22.52	good

4.2 Oslo station

For both the CMIP6 and the Cordex ensemble there were more than 5 models with the label 'good', so we only use the models that perform well.

Table 2. Evaluation results of the climate models considered for attribution analysis of 1min over Oslo. For each model, the expected temperature of a 1-in-200-year event is shown, along with the best estimate of the Sigma and Shape parameters and a 95% confidence interval for each, obtained via bootstrapping. The qualitative evaluation is shown in the right hand column. Based on overall suitability, the models are classified as good, reasonable or bad, shown by green, yellow and red highlights, respectively.

Model / Observations	Seasonal cycle	Spatial pattern	Sigma	Shape parameter	Event magnitude [°C]	Conclusion
Oslo			-3.26 (-3.84 ... -2.49)	-0.27 (-0.43 ... -0.12)	-23.1	
CMIP6 GCMs					**Threshold for return period 200yr event**	
ACCESS-ESM1-5	good	good	-2.61 (-3.21 ... -2.17)	-0.18 (-0.71 ... 0.020)	-23.98	good
CanESM5	bad	good	-4.56 (-5.26 ... -3.42)	-0.20 (-0.38 ... -0.040)	-39.92	bad, T>5
CMCC-ESM2	bad	good	-3.98 (-4.59 ... -3.15)	-0.30 (-0.51 ... -0.18)	-30.11	bad, T>5
CNRM-CM6-1-HR	good	good	-3.08 (-3.65 ... -2.29)	-0.24 (-0.47 ... -0.11)	-27.31	good
CNRM-CM6-1	good	good	-3.72 (-4.33 ... -3.05)	-0.21 (-0.45 ... -0.070)	-26.7	good
EC-Earth3	good	good	-3.15 (-3.63 ... -2.62)	-0.10 (-0.40 ... 0.030)	-33.84	bad, T>5
EC-Earth3-Veg	good	good	-3.20 (-3.71 ... -2.54)	-0.22 (-0.41 ... -0.090)	-30.78	bad, T>5
EC-Earth3-Veg-LR	good	good	-3.30 (-3.87 ... -2.62)	-0.21 (-0.36 ... -0.050)	-30.52	bad, T>5
FGOALS-g3	bad	bad	-4.62 (-5.32 ... -3.58)	-0.080 (-0.44 ... 0.080)	-52.94	bad, T>5
IPSL-CM6A-LR	bad	good	-5.84 (-6.86 ... -4.50)	-0.32 (-0.50 ... -0.14)	-42.58	bad, T>5
MIROC6	good	good	-3.33 (-3.86 ... -2.69)	-0.29 (-0.45 ... -0.17)	-24.97	good
MPI-ESM1-2-HR	good	good	-3.56 (-4.30 ... -2.45)	-0.21 (-0.43 ... 0.13)	-36.6	bad, T>5
MPI-ESM1-2-LR	good	good	-3.59 (-4.34 ... -2.78)	-0.41 (-0.60 ... -0.25)	-32.32	bad, T>5
MRI-ESM2-0	good	good	-3.59 (-4.15 ... -2.91)	-0.37 (-0.54 ... -0.21)	-23.8	good
NorESM2-LM	good	good	-4.03 (-4.67 ... -3.32)	-0.25 (-0.44 ... -0.13)	-27.36	reasonable
NorESM2-MM	good	good	-4.04 (-4.70 ... -3.23)	-0.25 (-0.48 ... -0.070)	-29.55	bad, T>5
CORDEX RCMs						
CanESM2_CLMcom-CCLM4-8-17	good	good	-2.97 (-3.51 ... -2.29)	-0.26 (-0.42 ... -0.11)	-22.45	good
CanESM2_GERICS-REMO2015	good	good	-5.75 (-6.74 ... -4.59)	-0.38 (-0.64 ... -0.27)	-28.8	bad, T>5
CNRM-CM5_CLMcom-CCLM4-8-17	good	good	-1.98 (-2.37 ... -1.60)	-0.11 (-0.32 ... 0.070)	-25.8	bad
CNRM-CM5_CLMcom-ETH-COSMO-crCLIM-v1-1	good	good	-2.98 (-3.62 ... -2.18)	-0.29 (-0.49 ... -0.030)	-23.87	good
CNRM-CM5_SMHI-RCA4	good	good	-3.28 (-4.00 ... -2.25)	-0.24 (-0.55 ... 0.020)	-34.42	bad, T>5
EC-EARTH_CLMcom-CCLM4-8-17	good	good	-2.95 (-3.42 ... -2.43)	-0.12 (-0.29 ... 0.050)	-25.47	good
EC-EARTH_CLMcom-ETH-COSMO-crCLIM-v1-1	good	good	-2.17 (-2.50 ... -1.79)	-0.12 (-0.28 ... 0.030)	-20.78	reasonable
EC-EARTH_DMI-HIRHAM5	good	good	-2.85 (-3.30 ... -2.28)	-0.18 (-0.38 ... 0.040)	-23.52	good
EC-EARTH_GERICS-REMO2015	good	good	-4.86 (-5.80 ... -3.80)	-0.43 (-0.74 ... -0.28)	-28.57	bad, T>5

EC-EARTH_ICTP-RegCM4-6	good	good	-3.00 (-3.55 ... -2.32)	-0.33 (-0.67 ... -0.20)	-20.13	good
EC-EARTH_IPSL-WRF381P	good	good	-3.56 (-4.11 ... -2.79)	-0.19 (-0.33 ... -0.020)	-26.41	good
EC-EARTH_KNMI-RACMO22E	good	good	-1.89 (-2.34 ... -1.40)	-0.30 (-0.59 ... -0.050)	-23.09	reasonable
EC-EARTH_MOHC-HadREM3-GA7-05	good	good	-3.00 (-3.45 ... -2.41)	-0.12 (-0.41 ... 0.020)	-35.01	bad, T>5
EC-EARTH_SMHI-RCA4	good	good	-3.69 (-4.63 ... -2.89)	-0.52 (-1.0 ... -0.30)	-25.46	reasonable
EC-EARTH_UHOH-WRF361H	good	good	-3.96 (-4.69 ... -2.97)	-0.14 (-0.42 ... 0.050)	-30.07	bad, T>5
IPSL-CM5A-LR_DMI-HIRHAM5	good	good	-3.45 (-4.29 ... -2.73)	-0.40 (-1.0 ... -0.24)	-25.3	good
IPSL-CM5A-LR_GERICS-REMO2015	good	good	-3.54 (-4.19 ... -2.89)	-0.11 (-0.33 ... 0.070)	-36.82	bad, T>5
IPSL-CM5A-LR_IPSL-WRF381P	good	good	-3.84 (-4.50 ... -3.03)	-0.21 (-0.43 ... -0.040)	-32.07	bad, T>5
IPSL-CM5A-LR_KNMI-RACMO22E	good	good	-2.74 (-3.17 ... -2.20)	-0.15 (-0.39 ... 0.010)	-29.8	bad, T>5
IPSL-CM5A-LR_SMHI-RCA4	good	good	-3.35 (-4.16 ... -2.59)	-0.39 (-0.82 ... -0.13)	-32.16	bad, T>5
MIROC5_CLMcom-CCLM4-8-17	good	good	-2.33 (-2.68 ... -1.85)	-0.22 (-0.39 ... -0.11)	-24.52	good
MIROC5_GERICS-REMO2015	good	good	-5.16 (-6.26 ... -3.67)	-0.32 (-0.48 ... -0.14)	-33.49	bad, T>5
HadGEM2-ES_CLMcom-CCLM4-8-17	good	good	-2.96 (-3.37 ... -2.52)	-0.15 (-0.39 ... -0.010)	-23.84	good
HadGEM2-ES_CLMcom-ETH-COSMO-crCLIM-v1-1	good	good	-2.71 (-3.16 ... -2.16)	-0.020 (-0.22 ... 0.16)	-25.83	reasonable
HadGEM2-ES_CNRM-ALADIN63	good	good	-2.99 (-3.52 ... -2.23)	-0.27 (-0.63 ... -0.020)	-22.22	good
HadGEM2-ES_GERICS-REMO2015	good	good	-5.91 (-6.82 ... -4.63)	-0.23 (-0.44 ... -0.050)	-30.96	bad, T>5
HadGEM2-ES_ICTP-RegCM4-6	good	good	-3.03 (-3.61 ... -2.27)	-0.16 (-0.36 ... 0.10)	-22.19	good
HadGEM2-ES_IPSL-WRF381P	good	good	-3.01 (-3.48 ... -2.44)	-0.18 (-0.35 ... -0.030)	-25.93	good
HadGEM2-ES_MOHC-HadREM3-GA7-05	good	good	-3.74 (-4.36 ... -3.03)	-0.22 (-0.40 ... -0.090)	-33.89	bad, T>5
HadGEM2-ES_SMHI-RCA4	good	good	-3.05 (-4.21 ... -2.36)	-0.46 (-1.1 ... -0.19)	-23.07	reasonable
HadGEM2-ES_UHOH-WRF361H	good	good	-4.08 (-4.81 ... -3.13)	-0.13 (-0.37 ... 0.060)	-27.8	reasonable
MPI-ESM-LR_CLMcom-CCLM4-8-17	good	good	-3.11 (-3.62 ... -2.51)	-0.24 (-0.52 ... -0.030)	-23.3	good
MPI-ESM-LR_CLMcom-ETH-COSMO-crCLIM-v1-1	good	good	-2.98 (-3.86 ... -2.34)	-0.17 (-0.56 ... 0.11)	-23.95	good
MPI-ESM-LR_CNRM-ALADIN63	good	good	-2.75 (-3.31 ... -2.22)	-0.39 (-0.64 ... -0.17)	-20.4	good
MPI-ESM-LR_DMI-HIRHAM5	good	good	-3.06 (-3.62 ... -2.47)	-0.17 (-0.38 ... 0.030)	-26.1	good

MPI-ESM-LR_GERICS-REMO2015	good	good	-5.38 (-6.34 ... -4.23)	-0.46 (-0.64 ... -0.33)	-30.91	bad, T>5
MPI-ESM-LR_ICTP-RegCM4-6	good	good	-1.94 (-2.38 ... -1.55)	-0.25 (-0.55 ... -0.020)	-16.32	bad, T>5
MPI-ESM-LR_IPSL-WRF381P	good	good	-2.76 (-3.18 ... -2.31)	-0.24 (-0.44 ... -0.060)	-24	good
MPI-ESM-LR_KNMI-RACMO22E	good	good	-2.34 (-2.75 ... -1.90)	-0.11 (-0.27 ... 0.060)	-28.39	bad, T>5
MPI-ESM-LR_MOHC-HadREM3-GA7-05	good	good	-3.58 (-4.34 ... -2.89)	-0.30 (-0.56 ... -0.10)	-33.79	bad, T>5
MPI-ESM-LR_MPI-CSC-REMO2009	good	good	-6.55 (-7.83 ... -5.28)	-0.35 (-0.63 ... -0.16)	-33.24	bad, T>5
MPI-ESM-LR_SMHI-RCA4	good	good	-3.13 (-3.68 ... -2.45)	-0.21 (-0.48 ... -0.020)	-30	bad, T>5
MPI-ESM-LR_UHOH-WRF361H	good	good	-2.93 (-3.42 ... -2.18)	-0.26 (-0.54 ... -0.070)	-24.27	good
NorESM1-M_CLMcom-ETH-COSMO-crCLIM-v1-1	good	good	-3.25 (-3.75 ... -2.55)	-0.33 (-0.52 ... -0.070)	-22.34	good
NorESM1-M_CNRM-ALADIN63	good	good	-2.70 (-3.14 ... -2.22)	-0.21 (-0.40 ... -0.070)	-22.31	good
NorESM1-M_GERICS-REMO2015	good	good	-6.36 (-7.41 ... -5.18)	-0.34 (-0.68 ... -0.23)	-33.31	bad, T>5
NorESM1-M_ICTP-RegCM4-6	good	good	-1.86 (-2.15 ... -1.50)	-0.070 (-0.43 ... 0.14)	-18.01	bad
NorESM1-M_IPSL-WRF381P	good	good	-3.12 (-3.62 ... -2.48)	-0.070 (-0.24 ... 0.12)	-28.94	bad, T>5
NorESM1-M_KNMI-RACMO22E	good	good	-2.39 (-2.84 ... -1.74)	-0.16 (-0.41 ... 0.040)	-27.12	reasonable
NorESM1-M_MOHC-HadREM3-GA7-05	good	good	-3.88 (-4.45 ... -3.11)	-0.31 (-0.47 ... -0.17)	-34.18	bad, T>5

5 Multi-method multi-model attribution

This section shows Probability Ratios and change in intensity ΔI for the CMIP6 and CORDEX models and also includes the values calculated from the fits with observations.

5.1 Area average

Table 3. Probability ratio and change in intensity: (a) from pre industrial climate to the present and (b) from the present to 2C above pre industrial climate, for the area average.

	a. Past vs. present		**b. Present vs. future**	
Model / Observations	**Probability ratio PR [-]**	**Change in intensity ΔI [°C]**	**Probability ratio PR [-]**	**Change in intensity ΔI [°C]**
ERA5 box	0.19 (0.023 ... 0.57)	4.3 (1.7 ... 6.7)	N/A	N/A
ACCESS-CM2	0.17 (0.046 ... 0.32)	4.5 (3.1 ... 6.0)	0.24 (0.075 ... 0.39)	2.6 (2.0 ... 3.1)
CanESM5	0.27 (0.097 ... 0.48)	3.4 (2.1 ... 4.5)	0.26 (0.022 ... 0.42)	2.5 (2.1 ... 2.9)

CNRM-CM6-1-HR	0.11 (0.023 ... 0.22)	5.2 (3.9 ... 6.7)	0.15 (0.022 ... 0.30)	2.3 (1.8 ... 2.8)
EC-Earth3	0.10 (0.015 ... 0.23)	6.9 (5.5 ... 8.6)	0.039 (0.00010 ... 0.16)	3.9 (3.4 ... 4.5)
EC-Earth3-Veg	0.098 (0.0080 ... 0.24)	6.5 (4.8 ... 7.9)	0.042 (0.00010 ... 0.16)	3.5 (2.9 ... 4.1)
INM-CM5-0	0.19 (0.010 ... 0.77)	3.3 (0.81 ... 5.8)	0.028 (0.00010 ... 0.16)	3.2 (2.5 ... 3.9)
MIROC6	0.16 (0.050 ... 0.42)	4.4 (2.3 ... 6.3)	0.23 (0.058 ... 0.40)	2.5 (1.8 ... 3.2)
MPI-ESM1-2-HR	0.35 (0.023 ... 0.97)	2.0 (0.11 ... 4.4)	0.21 (0.00010 ... 0.43)	2.2 (1.6 ... 3.0)
MPI-ESM1-2-LR	0.14 (0.018 ... 0.49)	4.1 (1.8 ... 6.0)	0.024 (0.00010 ... 0.13)	3.1 (2.5 ... 3.8)
NorESM2-LM	0.50 (0.090 ... 1.5)	1.6 (-0.94 ... 4.2)	0.67 (0.27 ... 0.99)	0.78 (0.030 ... 1.6)
NorESM2-MM	0.23 (0.044 ... 0.62)	3.9 (1.4 ... 6.5)	0.30 (0.073 ... 0.51)	2.3 (1.6 ... 3.1)
CanESM2_CLMcom-CCLM4-8-17	0.16 (0.0090 ... 0.41)	4.4 (2.8 ... 6.0)	0.079 (0.00010 ... 0.31)	2.4 (1.9 ... 3.0)
CanESM2_GERICS-REMO2015	0.21 (0.0090 ... 1.0e+4)	3.7 (1.3 ... 5.8)	0.20 (0.00010 ... 0.44)	2.3 (1.6 ... 2.9)
EC-EARTH_CLMcom-CCLM4-8-17	0.20 (0.0070 ... 1.0e+4)	3.2 (0.65 ... 6.3)	0.14 (0.00010 ... 0.51)	2.1 (1.3 ... 3.1)
EC-EARTH_DMI-HIRHAM5	0.080 (0.011 ... 0.20)	8.0 (5.5 ... 10)	0.11 (0.00010 ... 0.28)	3.6 (2.8 ... 4.5)
EC-EARTH_ICTP-RegCM4-6	0.12 (0.0020 ... 1.0e+4)	4.7 (0.66 ... 8.5)	0.0028 (0.00010 ... 0.31)	2.5 (1.5 ... 3.4)
EC-EARTH_IPSL-WRF381P	0.14 (0.0050 ... 1.0e+4)	4.5 (1.5 ... 7.2)	0.087 (0.00010 ... 0.36)	2.6 (1.7 ... 3.4)
EC-EARTH_KNMI-RACMO22E	0.078 (0.0080 ... 0.23)	7.0 (4.9 ... 9.6)	0.053 (0.00010 ... 0.20)	3.0 (2.2 ... 3.7)
EC-EARTH_MOHC-HadREM3-GA7-05	0.26 (0.016 ... 1.4)	3.7 (0.73 ... 6.4)	0.27 (0.00010 ... 0.53)	2.5 (1.7 ... 3.5)
EC-EARTH_SMHI-RCA4	0.084 (0.0060 ... 1.0e+4)	7.5 (4.0 ... 11)	0.060 (0.00010 ... 0.29)	3.5 (2.4 ... 4.5)
IPSL-CM5A-LR_DMI-HIRHAM5	0.16 (0.0080 ... 0.66)	3.6 (1.9 ... 5.3)	0.023 (0.00010 ... 0.16)	2.8 (2.3 ... 3.5)
IPSL-CM5A-LR_GERICS-REMO2015	0.20 (0.0010 ... 1.0e+4)	2.6 (0.71 ... 4.5)	0.054 (0.00010 ... 0.20)	2.4 (1.8 ... 3.0)
IPSL-CM5A-LR_IPSL-WRF381P	0.10 (0.013 ... 0.45)	5.0 (3.2 ... 6.7)	0.13 (0.00010 ... 0.35)	3.1 (2.3 ... 3.8)
MIROC5_GERICS-REMO2015	0.10 (0.0030 ... 1.0e+4)	6.0 (2.8 ... 9.4)	0.052 (0.00010 ... 0.36)	3.0 (1.9 ... 4.2)
HadGEM2-ES_CLMcom-CCLM4-8-17	0.27 (0.088 ... 0.55)	2.7 (1.2 ... 4.0)	0.30 (0.072 ... 0.48)	1.8 (1.4 ... 2.2)
HadGEM2-ES_CLMcom-ETH-COSMO-crCLIM-v1-	0.21 (0.042 ... 0.50)	3.2 (1.6 ... 4.6)	0.24 (0.00010 ... 0.42)	1.9 (1.5 ... 2.3)
HadGEM2-ES_IPSL-WRF381P	0.16 (0.022 ... 0.47)	3.8 (2.3 ... 5.3)	0.38 (0.099 ... 0.64)	1.6 (1.1 ... 2.1)

HadGEM2-ES_MOHC-HadREM3-GA7-05	0.20 (0.019 ... 0.43)	4.2 (2.7 ... 6.0)	0.16 (0.00010 ... 0.34)	2.9 (2.3 ... 3.5)
HadGEM2-ES_SMHI-RCA4	0.17 (0.024 ... 0.60)	4.1 (1.6 ... 6.3)	0.13 (0.00010 ... 0.35)	2.5 (1.8 ... 3.2)
MPI-ESM-LR_CLMcom-CCLM4-8-17	0.22 (0.0020 ... 1.0e+4)	3.9 (1.3 ... 7.1)	0.29 (0.00010 ... 0.63)	2.3 (1.4 ... 3.5)
MPI-ESM-LR_CLMcom-ETH-COSMO-crCLIM-v1-	0.20 (0.010 ... 0.51)	4.2 (2.3 ... 6.5)	0.26 (0.00010 ... 0.55)	2.4 (1.6 ... 3.4)
MPI-ESM-LR_DMI-HIRHAM5	0.23 (0.032 ... 0.66)	3.6 (1.3 ... 6.5)	0.19 (0.00010 ... 0.59)	2.6 (1.7 ... 3.7)
MPI-ESM-LR_GERICS-REMO2015	0.17 (0.027 ... 0.68)	3.8 (1.4 ... 6.0)	0.15 (0.0018 ... 0.36)	2.3 (1.6 ... 3.0)
MPI-ESM-LR_IPSL-WRF381P	0.17 (0.025 ... 0.57)	3.6 (1.5 ... 6.0)	0.16 (0.00010 ... 0.42)	2.3 (1.6 ... 3.0)
MPI-ESM-LR_KNMI-RACMO22E	0.22 (0.039 ... 0.57)	4.2 (1.7 ... 6.9)	0.30 (0.015 ... 0.57)	2.5 (1.7 ... 3.5)
MPI-ESM-LR_MPI-CSC-REMO2009	0.13 (0.0060 ... 1.0e+4)	3.9 (2.2 ... 5.7)	0.015 (0.00010 ... 0.14)	2.7 (1.8 ... 3.4)
MPI-ESM-LR_SMHI-RCA4	0.18 (0.0010 ... 1.0e+4)	3.7 (-0.59 ... 7.2)	0.073 (0.00010 ... 0.30)	2.9 (2.1 ... 3.9)
MPI-ESM-LR_UHOH-WRF361H	0.23 (0.041 ... 0.88)	4.2 (0.50 ... 7.9)	0.21 (0.00010 ... 0.51)	3.0 (1.8 ... 4.3)
NorESM1-M_CLMcom-ETH-COSMO-crCLIM-v1-1	0.41 (0.073 ... 1.2)	1.9 (-0.38 ... 4.4)	0.51 (0.15 ... 0.85)	1.2 (0.41 ... 2.0)
NorESM1-M_GERICS-REMO2015	0.27 (0.036 ... 1.0e+4)	2.6 (-0.49 ... 5.7)	0.23 (0.00010 ... 0.57)	1.9 (0.84 ... 2.8)
NorESM1-M_ICTP-RegCM4-6	0.18 (0.021 ... 0.81)	3.4 (0.74 ... 6.1)	0.23 (0.00010 ... 0.53)	1.7 (0.87 ... 2.4)
NorESM1-M_MOHC-HadREM3-GA7-05	0.27 (0.061 ... 0.94)	3.0 (0.13 ... 5.7)	0.28 (0.00010 ... 0.61)	1.9 (1.0 ... 2.8)

5.2 Oslo station

Table 4. *Probability ratio and change in intensity: (a) from preindustrial climate to the present and (b) from the present to 2C above preindustrial, for the Oslo region.*

	a. Past vs. present		**b. Present vs. future**	
Model / Observations	**Probability ratio PR [-]**	**Change in intensity ΔI [°C]**	**Probability ratio PR [-]**	**Change in intensity ΔI [°C]**
Oslo	0.023 (0.000044 ... ∞)	5.0 (2.5 ... 8.1)	N/A	N/A
ACCESS-ESM1-5	0.032 (0.0 ... 1.0e+4)	4.5 (2.9 ... 5.8)	0.0032 (0.00010 ... 0.15)	2.4 (1.9 ... 2.9)

CNRM-CM6-1-HR	0.039 (0.0 ... 1.0e+4)	4.3 (2.7 ... 5.8)	0.044 (0.00010 ... 0.28)	1.8 (1.3 ... 2.3)
CNRM-CM6-1	0.056 (0.0 ... 1.0e+4)	4.9 (3.1 ... 6.7)	0.11 (0.00010 ... 0.40)	2.1 (1.4 ... 2.8)
MIROC6	0.025 (0.0 ... 1.0e+4)	5.2 (2.7 ... 7.9)	0.00010 (0.00010 ... 0.15)	2.7 (1.9 ... 3.5)
MRI-ESM2-0	0.056 (0.0 ... 1.0e+4)	4.9 (2.8 ... 7.3)	0.14 (0.00010 ... 0.41)	2.4 (1.7 ... 3.1)
CanESM2_CLMcom-CCLM4-8-17	0.067 (0.0 ... 1.0e+4)	2.9 (1.8 ... 4.1)	0.016 (0.00010 ... 0.31)	1.7 (1.2 ... 2.1)
CNRM-CM5_CLMcom-ETH-COSMO-crCLIM-v1-1	0.044 (0.0 ... 1.0e+4)	3.4 (0.93 ... 6.1)	∞ (0.00010 ... 0.41)	2.2 (1.3 ... 3.1)
EC-EARTH_CLMcom-CCLM4-8-17	0.23 (0.0070 ... 4.0)	2.6 (0.45 ... 4.9)	0.35 (0.00010 ... 0.64)	1.4 (0.80 ... 2.1)
EC-EARTH_DMI-HIRHAM5	0.028 (0.0 ... 1.0e+4)	5.8 (3.4 ... 7.9)	0.00050 (0.00010 ... 0.20)	2.9 (2.1 ... 3.6)
EC-EARTH_ICTP-RegCM4-6	0.033 (0.0 ... 1.0e+4)	3.5 (-0.13 ... 6.3)	0.00010 (0.00010 ... 0.13)	2.0 (0.78 ... 2.9)
EC-EARTH_IPSL-WRF381P	0.12 (0.0020 ... 1.0e+4)	3.5 (0.90 ... 6.5)	0.096 (0.00010 ... 0.43)	2.3 (1.5 ... 3.2)
IPSL-CM5A-LR_DMI-HIRHAM5	0.013 (0.0 ... 1.0e+4)	5.5 (3.3 ... 7.9)	0.00010 (0.00010 ... 0.12)	2.3 (1.6 ... 3.1)
MIROC5_CLMcom-CCLM4-8-17	0.13 (0.0010 ... 1.0e+4)	1.9 (-0.27 ... 3.8)	0.13 (0.00010 ... 0.47)	1.3 (0.65 ... 1.8)
HadGEM2-ES_CLMcom-CCLM4-8-17	0.13 (0.0010 ... 1.0e+4)	3.1 (1.5 ... 4.9)	0.23 (0.00010 ... 0.60)	1.6 (1.1 ... 2.1)
HadGEM2-ES_CNRM-ALADIN63	0.11 (0.0030 ... 1.0e+4)	2.2 (0.35 ... 4.0)	0.13 (0.00010 ... 0.57)	1.1 (0.63 ... 1.6)
HadGEM2-ES_ICTP-RegCM4-6	0.14 (0.0020 ... 1.0e+4)	3.1 (1.1 ... 4.8)	0.14 (0.00010 ... 0.58)	1.6 (0.92 ... 2.3)
HadGEM2-ES_IPSL-WRF381P	0.081 (0.0 ... 1.0e+4)	3.7 (2.1 ... 5.4)	0.32 (0.00010 ... 0.67)	1.3 (0.79 ... 1.9)
MPI-ESM-LR_CLMcom-CCLM4-8-17	0.048 (0.0 ... 1.0e+4)	3.8 (1.5 ... 5.7)	0.019 (0.00010 ... 0.56)	2.1 (1.1 ... 2.8)
MPI-ESM-LR_CLMcom-ETH-COSMO-crCLIM-v1-1	0.094 (0.0010 ... 1.0e+4)	3.1 (1.3 ... 5.0)	∞ (0.00010 ... 0.39)	2.2 (1.5 ... 3.0)
MPI-ESM-LR_CNRM-ALADIN63	0.034 (0.0 ... 1.0e+4)	2.5 (1.2 ... 3.7)	0.0052 (0.00010 ... 0.31)	1.6 (0.96 ... 2.3)
MPI-ESM-LR_DMI-HIRHAM5	0.070 (0.0 ... 1.0e+4)	4.2 (1.9 ... 6.5)	0.089 (0.00010 ... 0.38)	3.0 (2.3 ... 3.7)
MPI-ESM-LR_IPSL-WRF381P	0.11 (0.0010 ... 1.0e+4)	2.3 (0.43 ... 4.0)	0.00067 (0.00010 ... 0.36)	1.8 (1.1 ... 2.5)
MPI-ESM-LR_UHOH-WRF361H	0.061 (0.0010 ... 1.0e+4)	3.1 (0.90 ... 5.6)	0.00010 (0.00010 ... 0.32)	2.1 (1.2 ... 3.0)
NorESM1-M_CLMcom-ETH-COSMO-crCLIM-v1-1	0.12 (0.0010 ... 1.0e+4)	1.8 (-1.0 ... 4.5)	0.000034 (0.00010 ... 0.53)	1.6 (0.74 ... 2.3)

NorESM1-M_CNRM-ALADIN63	0.11 (0.0 ... 1.0e+4)	2.5 (0.030 ... 4.7)	0.065 (0.00010 ... 0.52)	1.5 (0.78 ... 2.1)

6 Hazard synthesis

For the event definitions described above we evaluate the influence of anthropogenic climate change on the events by calculating the probability ratio as well as the change in intensity using observations and climate models. Models which do not pass the validation tests described above are excluded from the analysis. The aim is to synthesise results from models that pass the evaluation along with the observations-based products (here ERA5), to give an overarching attribution statement. Figs. 6-9 show the changes in probability and intensity for the observations (blue) and models (red). Before combining them into a synthesised assessment, a term to account for intermodel spread is added (in quadrature) to the natural variability of the models. This is shown in the figures as white boxes around the light red bars. The dark red bar shows the model average, consisting of a weighted mean using the (uncorrelated) uncertainties due to natural variability plus the term representing intermodel spread (i.e., the inverse square of the white bars). Observation-based products and models are combined into a single result in two ways. Firstly, we neglect common model uncertainties beyond the intermodel spread that is depicted by the model average, and compute the weighted average of models (dark red bar) and observations (dark blue bar): this is indicated by the magenta bar. As, due to common model uncertainties, model uncertainty can be larger than the intermodel spread, secondly, we also show the more conservative estimate of an unweighted, direct average of observations (dark red bar) and models (dark blue bar) contributing 50% each, indicated by the white box around the magenta bar in the synthesis figures.

For the area average, the climate models agree well with the observed change: the model average is entirely within the uncertainty bounds of the intensity change and probability ratio of ERA5. Therefore, the models confine the results from observations, and we use the weighted average between observations and models (purple bar) to obtain a synthesised value. The synthesised change in intensity is 4.18 ℃ (95% confidence interval; 2.72 ℃ to 5.60 ℃). This means that a 1-in-15 year cold wave is nowadays about 4 ℃ warmer than it would have been without climate change (i.e 1.2℃ cooler climate). The probability ratio is 0.191 (0.139 to 0.229), which means that such a cold wave happens nowadays about 0.2 times as often as without climate change - in other words, these cold waves have become about 5 times less frequent (Fig. 6). We expect such cold waves to become even less cold and less frequent in a future climate that is 0.8 ℃ warmer than today: with synthesised results (Fig. 7) showing another 2.49 ℃ (1.348 ℃ to 3.49 ℃) warmer and a Probability Ratio of 0.207 (0.052 to 0.750) which means again about 5 times less frequent than today. A sensitivity analysis of replacement of PR upper and lower bound values of 10,000 by 100,000 and 0.0001 by 0.00001 shows that the main conclusions are robust.

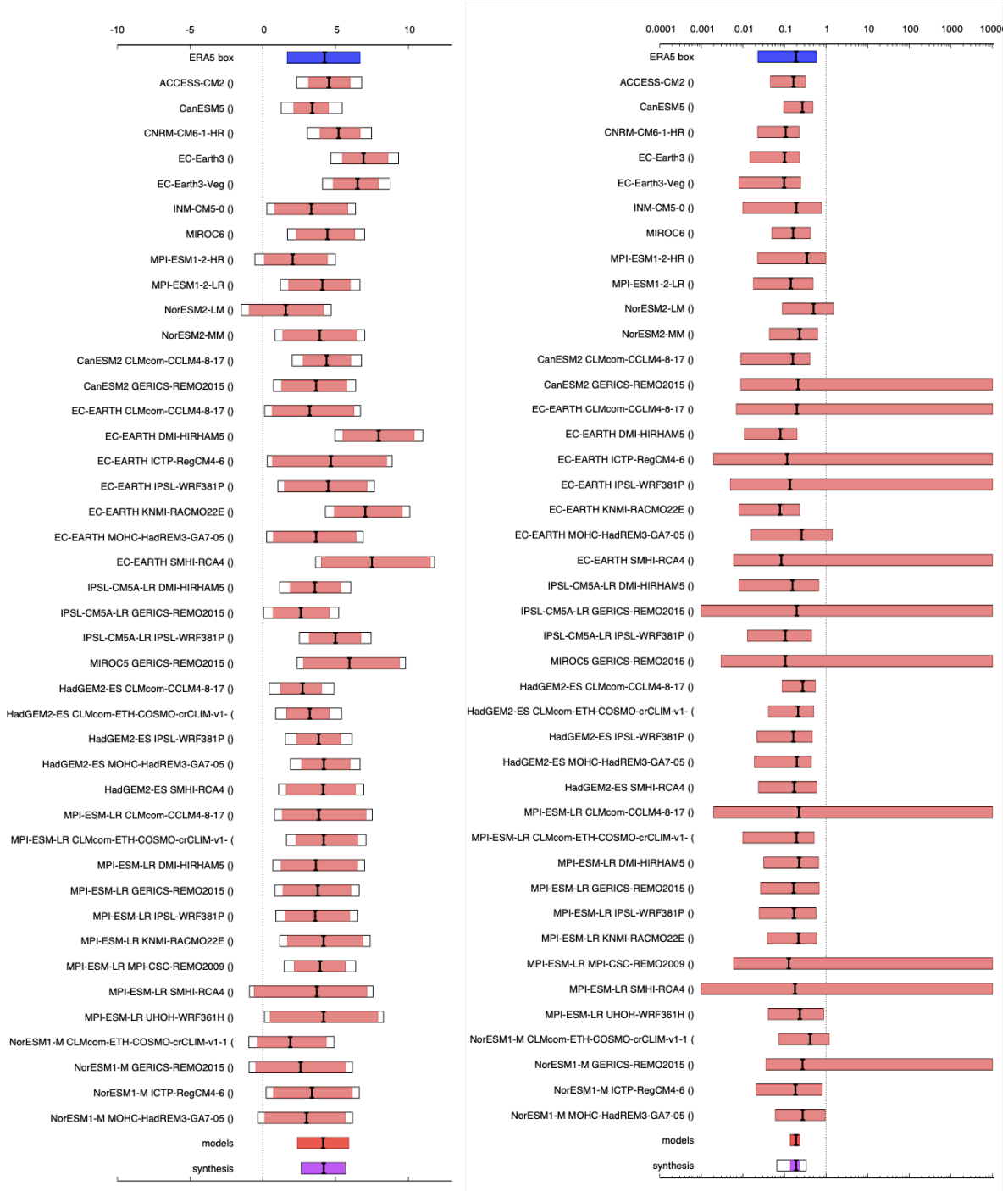

Figure 6: Synthesis of intensity change (left) and probability ratios (right), when comparing the box average over Fennoscandia with a 1.2°C cooler climate.

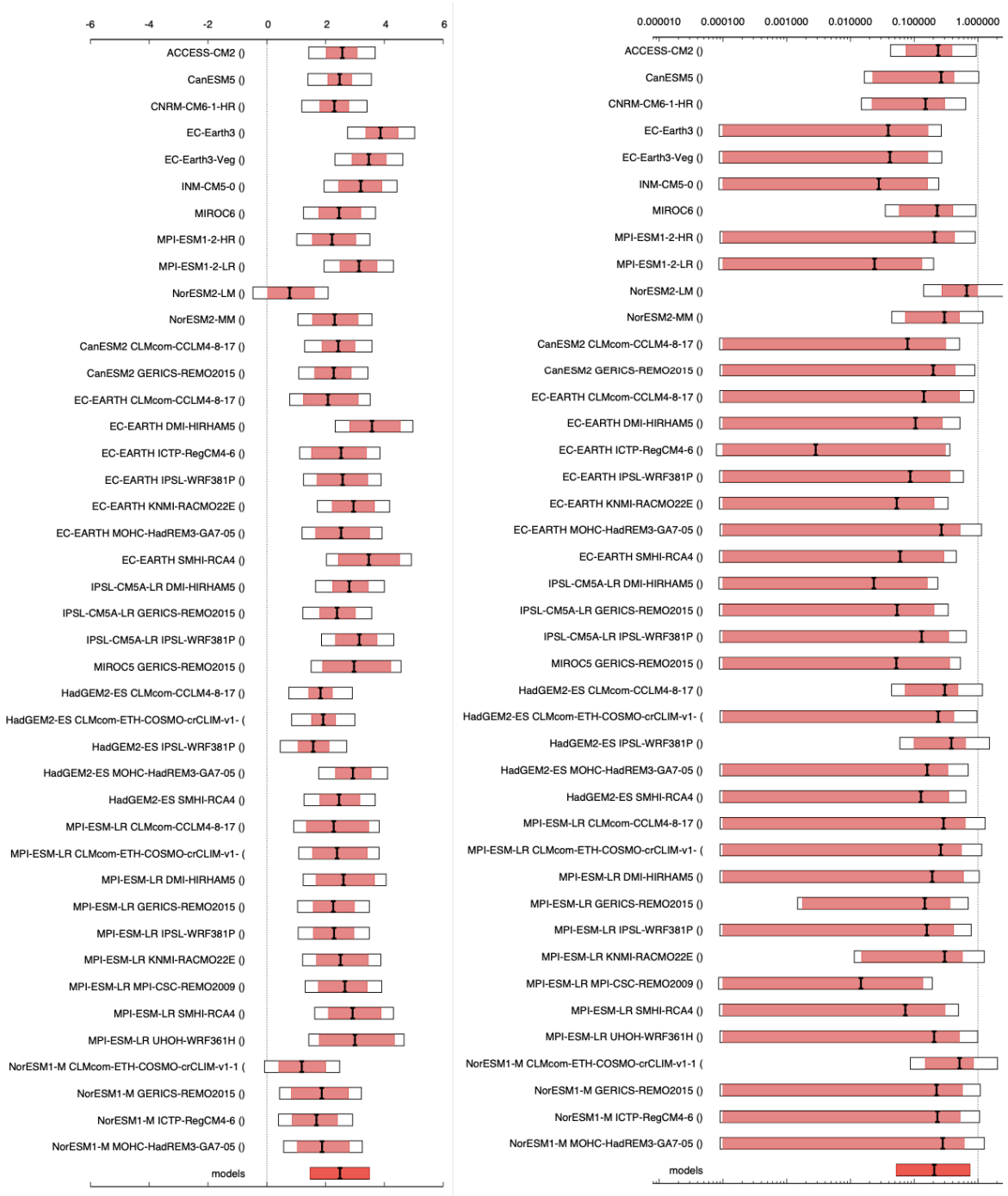

Figure 7: Synthesis of intensity change (left) and probability ratios (right), when comparing the box average over Scandinavia with a 0.8°C warmer climate.

For the Oslo station area, models agree again well with the observed change (Fig. 8): the model average is entirely within the uncertainty bounds of the probability ratio of Oslo station data, and almost entirely for the intensity change (Oslo range between 2.48 ℃ and 8.09 ℃ and model average range between 2.44 ℃ and 4.51℃). The overlap is big enough to use the weighted average between observations and models (purple bar). The synthesised change in intensity is 3.67 °C (95% confidence interval 2.70 ℃ to 4.65 ℃). This means that such a cold wave is nowadays about 4 ℃ warmer than without climate change. The probability ratio is 0.0853 (0.0269 to 0.611), which means that such cold

waves have become about 12 times less frequent. We expect such cold waves to become even less cold and less frequent in a future climate that is 0.8 ℃ warmer than today (Fig. 9): another 1.91 ℃ (1.15 ℃ to 2.67 ℃) warmer and the Probability Ratio is 0.00696 (0.000258 to 0.0183) which means about 144 times less frequent. A sensitivity analysis of the probability ratio to replacement of values of 10,000 by 100,000, 0.0001 by 0.00001 and best estimates of 0.0002 by 0.00002 shows that the main conclusions are robust; the PR between past-present changes from 12 to 10 times less likely, and the PR between future and present changes from 144 to 271 times less likely.

Because of the many very large (infinity) and very small (zero) values for the Probability Ratio, we focus on the communication of intensity change. This is similar to the approach taken in communication of many heat wave studies conducted by WWA. We emphasize however that the PR results are robust as well. Combining physical knowledge and synthesis results, and because of the clear and significant results, we communicate best estimates for all metrics, with the exception of the PR between present and future. There we communicate the qualitative result, that cold spells will become even less frequent, without emphasis on the quantitative result.

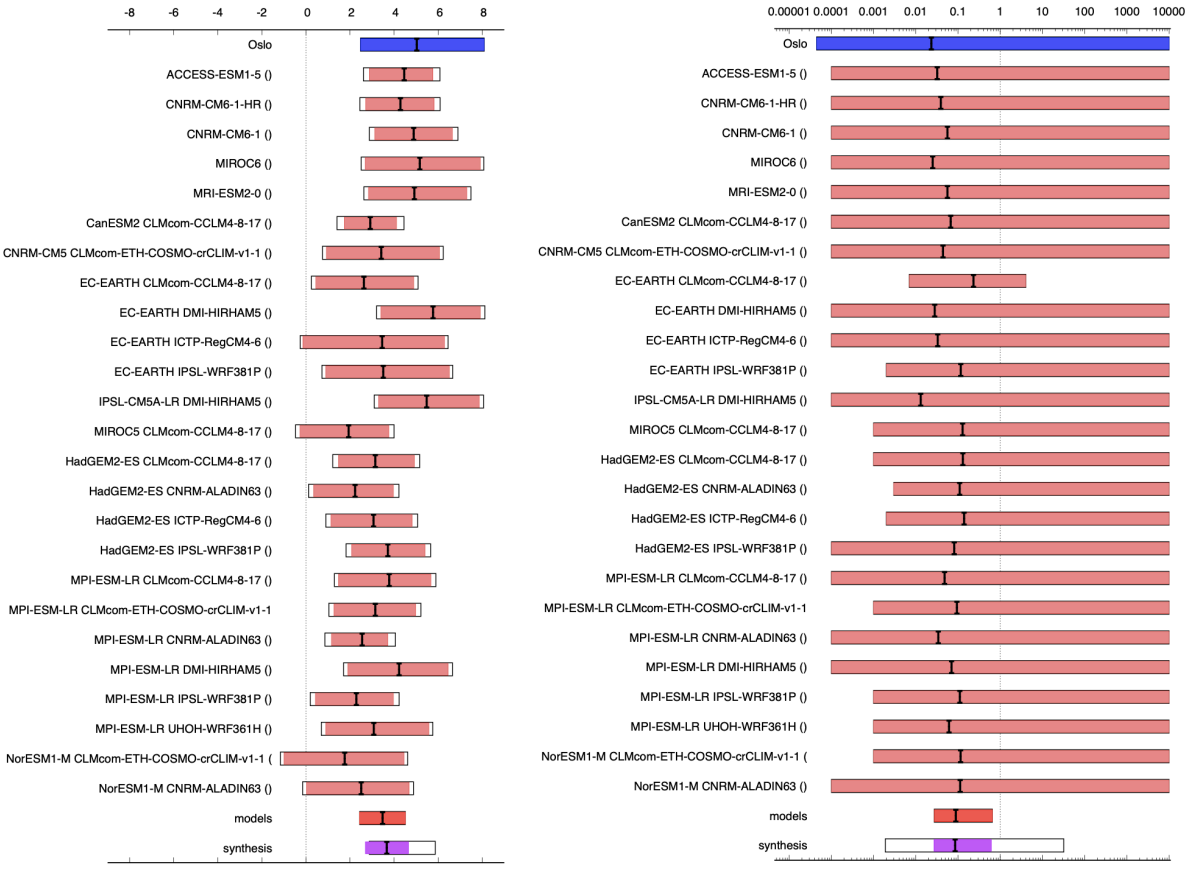

Figure 8: Synthesis of intensity change (left) and probability ratios (right), when comparing the Oslo station location with a 1.2°C cooler climate.

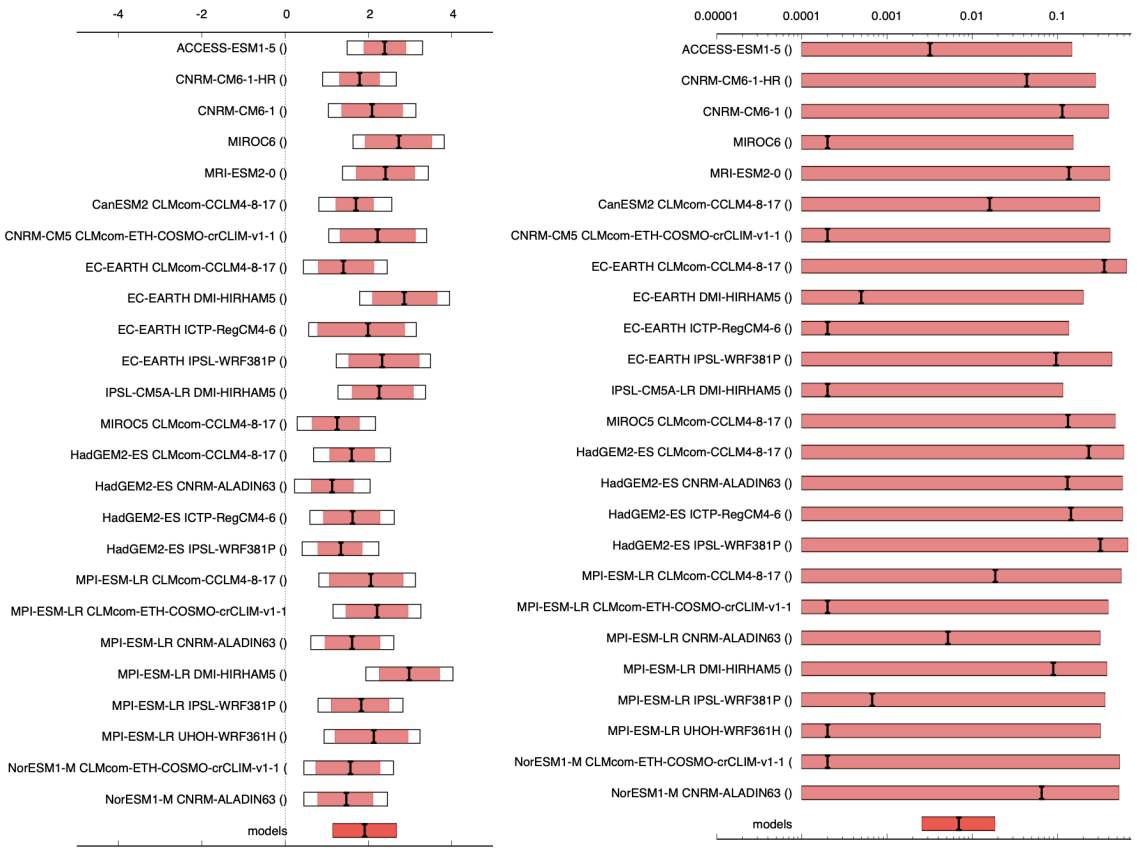

Figure 9: Synthesis of intensity change (left) and probability ratios (right), when comparing the Oslo station location with a 1.2°C warmer climate.

7 Vulnerability and exposure

Vulnerability and exposure are key components of the disaster risk equation alongside the hazard. For any hydrometeorological event, understanding the context in which the shock occurred and underlying vulnerabilities and exposure patterns can help explain the impacts that were felt. Whilst Fennoscandia is historically no stranger to cold temperatures, these periods of extreme cold are becoming less likely and with decreasing experience, preparedness may decrease. It is essential that individual and system preparedness to extreme cold continue to be emphasised.

Intersecting vulnerabilities

Particular socio-demographic groups tend to be more vulnerable and therefore suffer more consequences from cold waves or cold temperatures in general. People can be at higher risk of extreme cold due to physiological factors, including pregnant women, older people, and young children (Lakhoo 2022). Other groups might be at a higher risk due to certain contextual or socio-economic conditions, such as outdoor workers, people living in shelters, homeless people, ethnic minority groups, or people living in homes without adequate electricity or heat (ibid.). A previous study focussing on heat and cold waves from 1990 - 2002 in Stockholm County, Sweden, highlighted groups with stronger associations to mortality during cold spells for this region. Groups at

higher risk were found to be older populations (> 65 years old), individuals with a background of substance abuse and admission for mental health, and individuals with pre-existing myocardial infarction (heart attack) (Rocklöv et al. 2014). In addition, individuals living in wealthier municipalities were found to be at higher risk, which could be explained by the less energy efficient, older housing present in wealthier municipalities in Stockholm (ibid.). Lower-income populations are also at higher risk due a lack of warm clothes and inability to afford energy costs, especially when intersecting with energy crises and higher prices as during this cold wave. Finally, during this particular event, anecdotal reports emerged of higher use of wood burning stoves for longer periods, which caused more fires than usual, which in turn also impacts human health and the environment through the emissions of particulate matter (Salhberg et al. 2022). Impacts on human health resulting from this particular event - ranging from frost damage to mortality - have not been yet reported; it will take time for the full impacts to become evident.

Shelter

Homelessness has also been noted as a significant risk factor in severe impacts from cold waves (notably see Bezgrebelna et al. 2021) and is systemic in all three countries. In Fennoscandia, Sweden contains the highest rate with 3.5 homeless people per 1000 inhabitants, compared to approximately 1.2 homeless people/1000 inhabitants in Finland and Norway (Benjaminsen et al. 2020). In Finland and Norway, a decrease in homelessness has been observed over the past decade, but in Sweden, homelessness has been increasing in recent years (ibid.). In Sweden, temporary shelters for homeless are, in principle available, in most municipalities, organised through the social administration or supported by civil society organisations; nevertheless, some people in need may not have the capacity to seek such assistance. Often, people experiencing homelessness are also experiencing substance abuse problems and/or mental illness (ibid.), which results in compounding risks from extreme cold (e.g. less protection from cold exposure, reduced perception of health risks with substance use, etc.) (Rocklöv et al. 2014). In addition to the homeless citizens, a particularly vulnerable group may be visitors from other countries in the EU and beyond who work temporary, low-wage, or informal jobs, and often depend on precarious shelters (Waggman et al. 2019).

Energy, water, and transportation systems

Cold waves put pressure on energy systems by reducing the supply on one hand (e.g. through downed power lines and lower wind) and increasing the demand. Indeed, this cold wave had significant impacts on the electricity grid across the region with power lines down and households cut from the grid for multiple days. For instance, in Northern Sweden, 4,000 households were left without electricity (The Independent 2024). The cold wave also compounded the ongoing energy crisis as energy demand and prices soared in Northern Europe during this period and providers needed to expand the system to meet this pressure. In Finland, electricity prices rose up to record levels on the 5th of January due to exceptional weather conditions and failures of Finnish power plants (Yle, 2024). The prices during the day were exceptionally high for Finland where electricity prices are generally modest compared to other European countries (Eurostat 2023). Gas demand also increased in the region due to the cold wave - for example, the Finnish government made a rapid order for more liquid natural gas to balance demand (Reuters 2024). The coldwave also had significant impacts on this system, with road closures and public transport disruptions notably hitting the newly electrified bus system in Oslo whose batteries and charging speeds were affected by the cold temperatures (Khastenkova, 2024).

As for all shocks, particularly vulnerable people and households will be differentially impacted by these electricity cuts, price increases, and public transportation disruptions. Notably, fuel and energy poverty is an important equity issue which becomes particularly visible during cold periods (Boardman 2013, Marchand et al. 2019) - households living in low quality housing stock are likely to have higher heating bills because of the lack of insulation of the building and are more likely to be economically disadvantaged and more vulnerable to price hikes. Similarly, transportation issues have differential impacts on certain groups of people whose livelihoods depend on the functioning of these networks and may be particularly vulnerable when these are disrupted.

Cold wave action planning, preparedness, and response

Sweden, Norway, and Finland all have resourced national meteorological services which provide forecasting and certain forms of warning information. For example, the Swedish Meteorological and Hydrological Institute (SMHI) launched "impact-based forecasting" in 2021 and issued warnings and advisories through public service media, including recommendations on prevention measures. SMHI, as well as the Finnish Meteorological Institute (FMI) and the Norwegian Meteorological Institute all provide 10-day forecasts via apps, website and news media – and more specific weather alerts and warnings. The January 2024 cold wave in Fennoscandia was forecasted and disseminated days ahead in all three countries. However, accurate warning systems do not always translate into early action - and after-action reviews are essential to understand the effectiveness of the warnings received by different vulnerable groups.

The deployment of cold wave preparedness plans can significantly reduce the risk of impacts during cold waves. These types of plans generally include a monitoring of temperatures and different activities undertaken to support particularly vulnerable people during extreme cold periods. Both long and short-term prevention and preparedness measures are essential for this. The three countries in the study area are no stranger to cold - people, housing and facilities are generally geared to cold winter conditions - and systems and programmes exist to prepare and respond to these types of events. For example, Finland has training programmes about cold wave risks for individuals and professional bodies, particularly in the health sector (Laadi et al. 2013). During the event, the Oslo municipality focused on ensuring the safety of those who sleep outdoors, and kept Oslo Central Station open on the night of the 6th so that people could have a warm place to sleep (Aftenposten 2024). Both Finnish and Swedish authorities have stepped up messaging for preparedness at the household level in case of crises or emergencies in general, including recommendations for managing during power outages and cold conditions (MSB 2021, Pelastustoimi n.d.). In addition, the Swedish National Knowledge Centre for Climate Change Adaptation offers training courses to regional/municipal planners on adaptation, including, e.g., heatwaves and, potentially, cold snaps (and runs the Swedish Portal for Climate Change Adaptation).

The Swedish Civil Contingencies Agency (MSB), in collaboration with The Swedish Association of Local Authorities and Regions, has issued a short handbook on local (municipal level) preparedness for low temperatures (MSB 2022). The handbook points to joint Swedish-Finnish-Danish technical recommendations for "Smart practices in cold climates (2018)" in relation to emergency operations in cold climates but it does not specifically address risk reduction, warning efforts and assistance

towards vulnerable groups. Sweden's National Strategy for Climate Change Adaptation - due for its regular 5-year update by 2023 - does not refer to cold snaps or low temperatures.

V&E conclusions

Even if global temperatures are increasing and that cold wave frequency may be decreasing generally in the region, events such as this one can serve as powerful reminders that extreme cold waves are still possible and may, in fact, have more severe impacts than similar events in the past, if risk perception and preparedness become lower as people have less experience and memories of coldwaves. Intersecting vulnerabilities related to poverty and socio-economic demographics make certain people and communities more at risk. Housing, energy, water, and health systems must be prepared and resilient to weather-related shocks, and preparedness and response plans are critical to ensuring that vulnerable people are protected from the cascading impacts of these types of events. After-action reviews and research may illuminate questions and recommendations for the future, notably about the effectiveness of certain measures, and recommendations to ensure greater resilience.

Data availability and Acknowledgments

Almost all data is available via the Climate Explorer.
This study benefited from the ESPRI computing and data centre (https://mesocentre.ipsl.fr) which is supported by CNRS, Sorbonne Université, Ecole Polytechnique and CNES as well as through national and international grants.

References

All references are given as hyperlinks in the text.

Date
29/01/2024

Supplementary figures

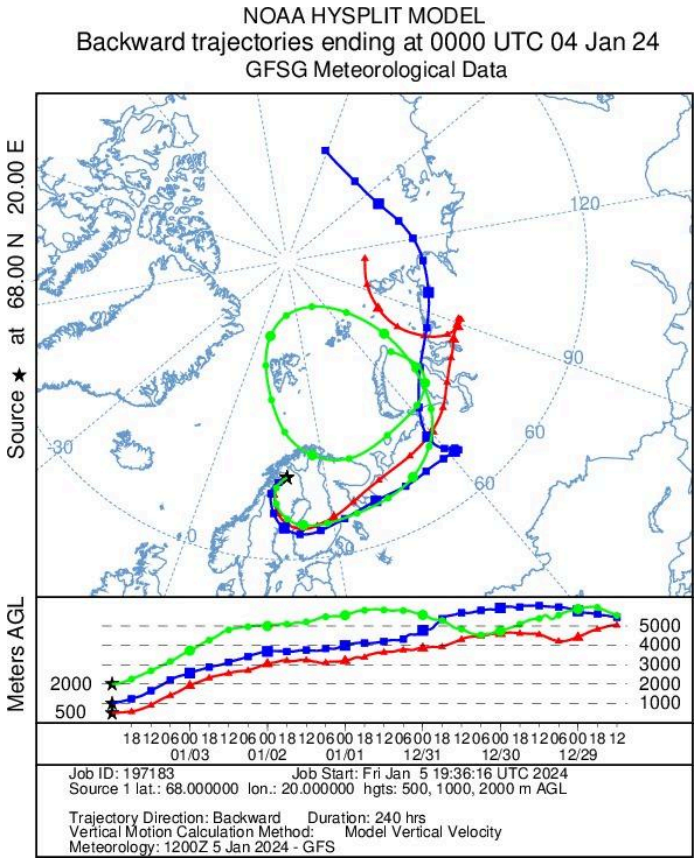

Figure A1: 5-day back-trajectories of particles arriving near Abisko (20E, 68N), on 4/1/2024 00 UTC, at altitudes of 500m, 1000m and 2000m, using the NOAA HySplit trajectory model (https://www.ready.noaa.gov/hypub-bin/trajtype.pl) and the GFS archive.

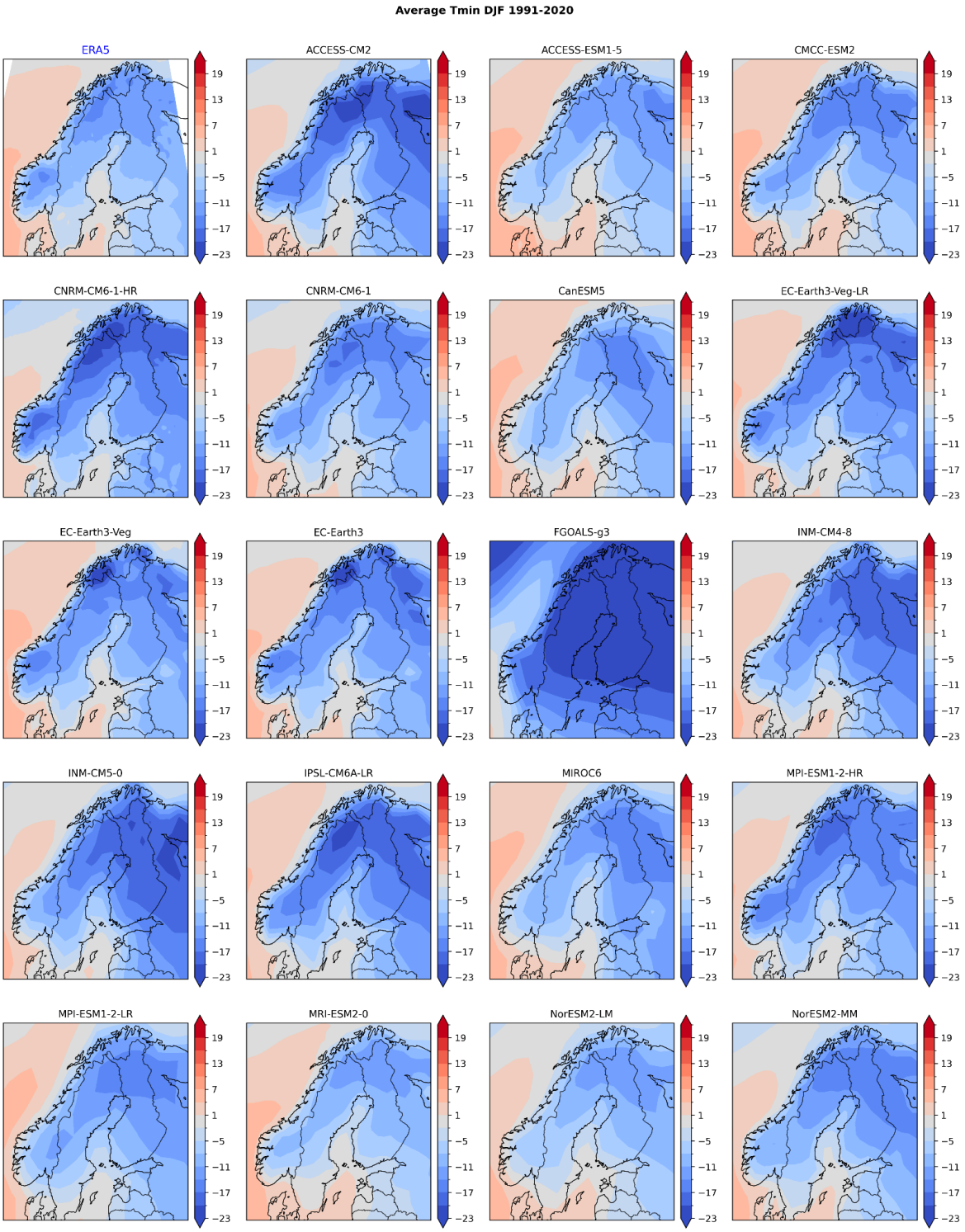

Figure A2: Average minimum temperature for December-February over a climatological period of 1991-2020 of ERA5 and CMIP6 models.

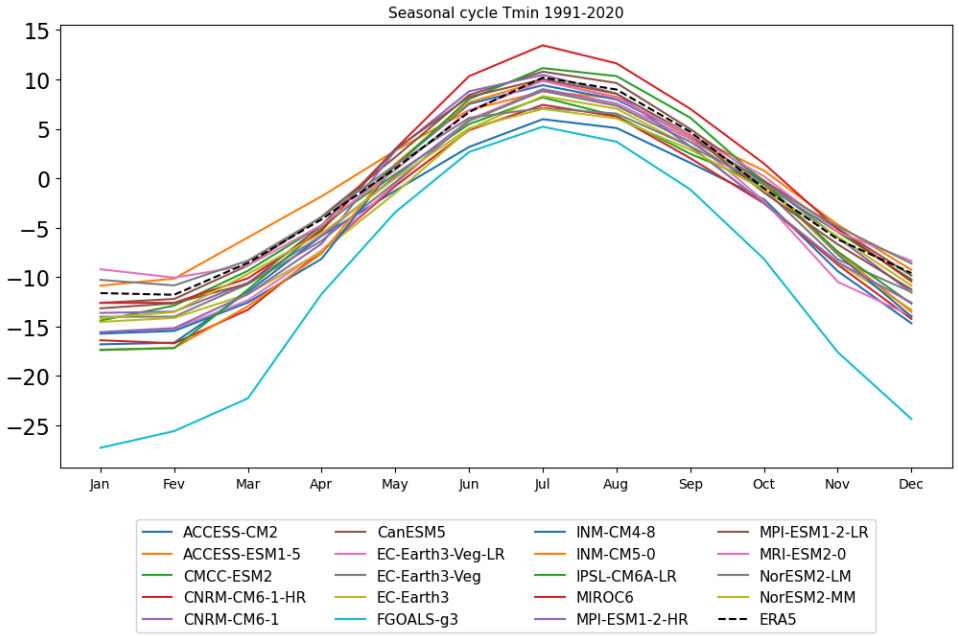

Figure A3: Seasonal cycle of average minimum temperature over a climatological period of 1991-2020 of ERA5 and CMIP6 models over the study area (red box of Figure 1a).

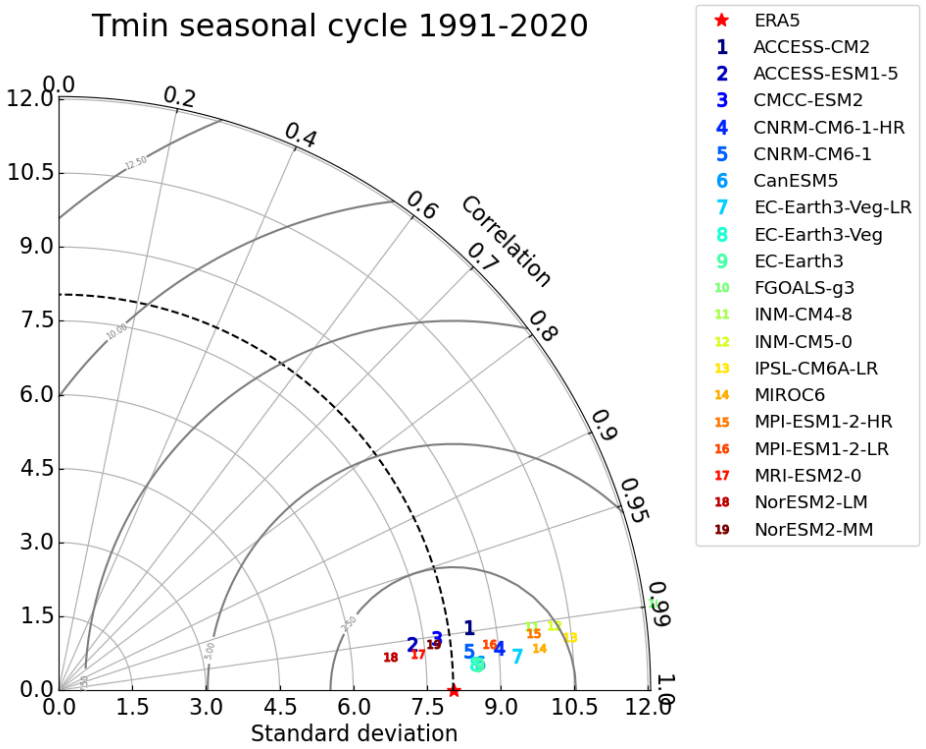

Figure A4: Taylor diagrams used to evaluate seasonal cycle average minimum temperature over the study area in the CMIP6 ensemble against the ERA5 reference. The azimuthal angle corresponds to the Pearson correlation coefficient between the simulated climatology and the reference climatology, which quantifies how well the two patterns match; the radial distance from the origin indicates the standard deviation, which measures the amplitude of the pattern.

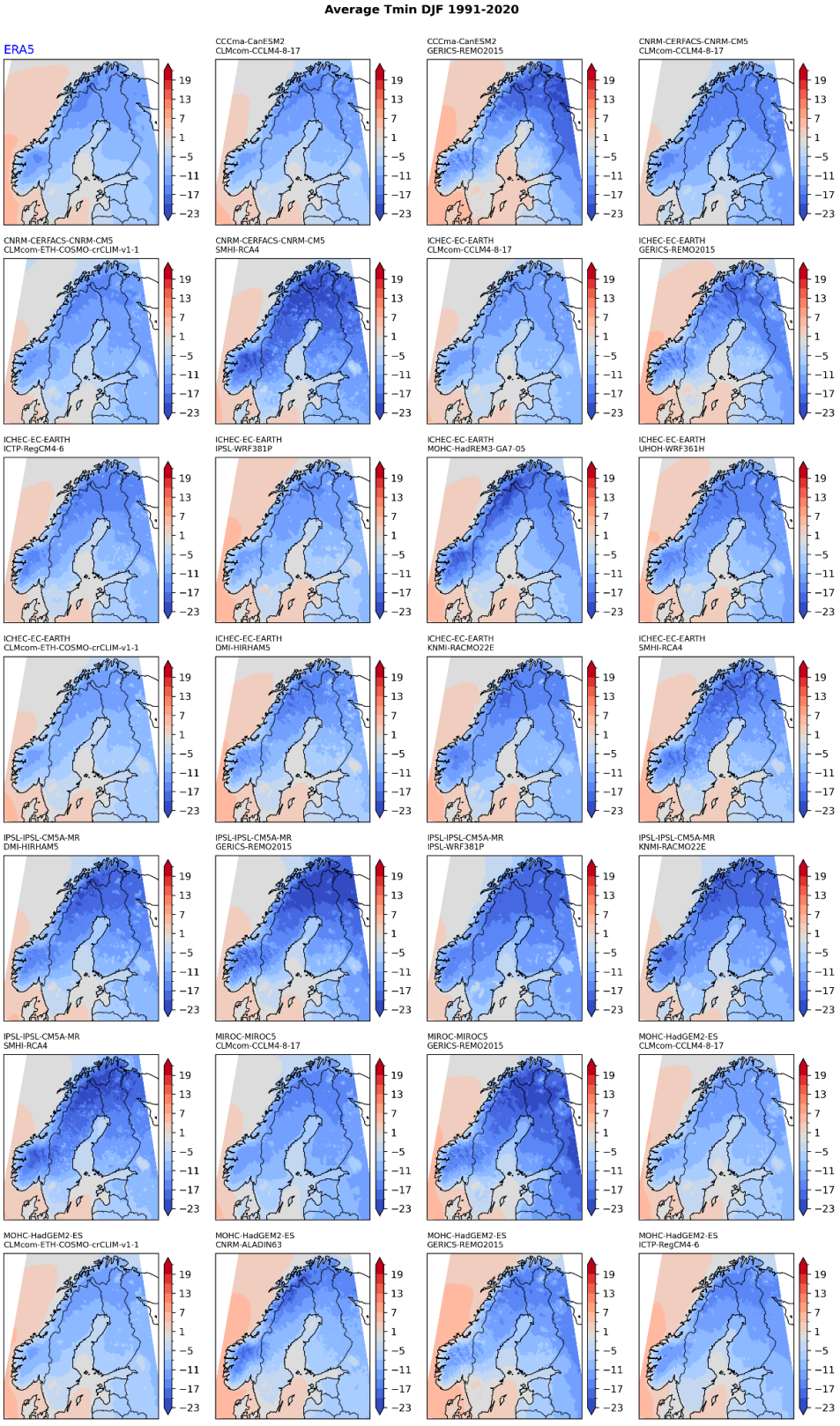

Figure A5. Same as A2 but for CORDEX models.

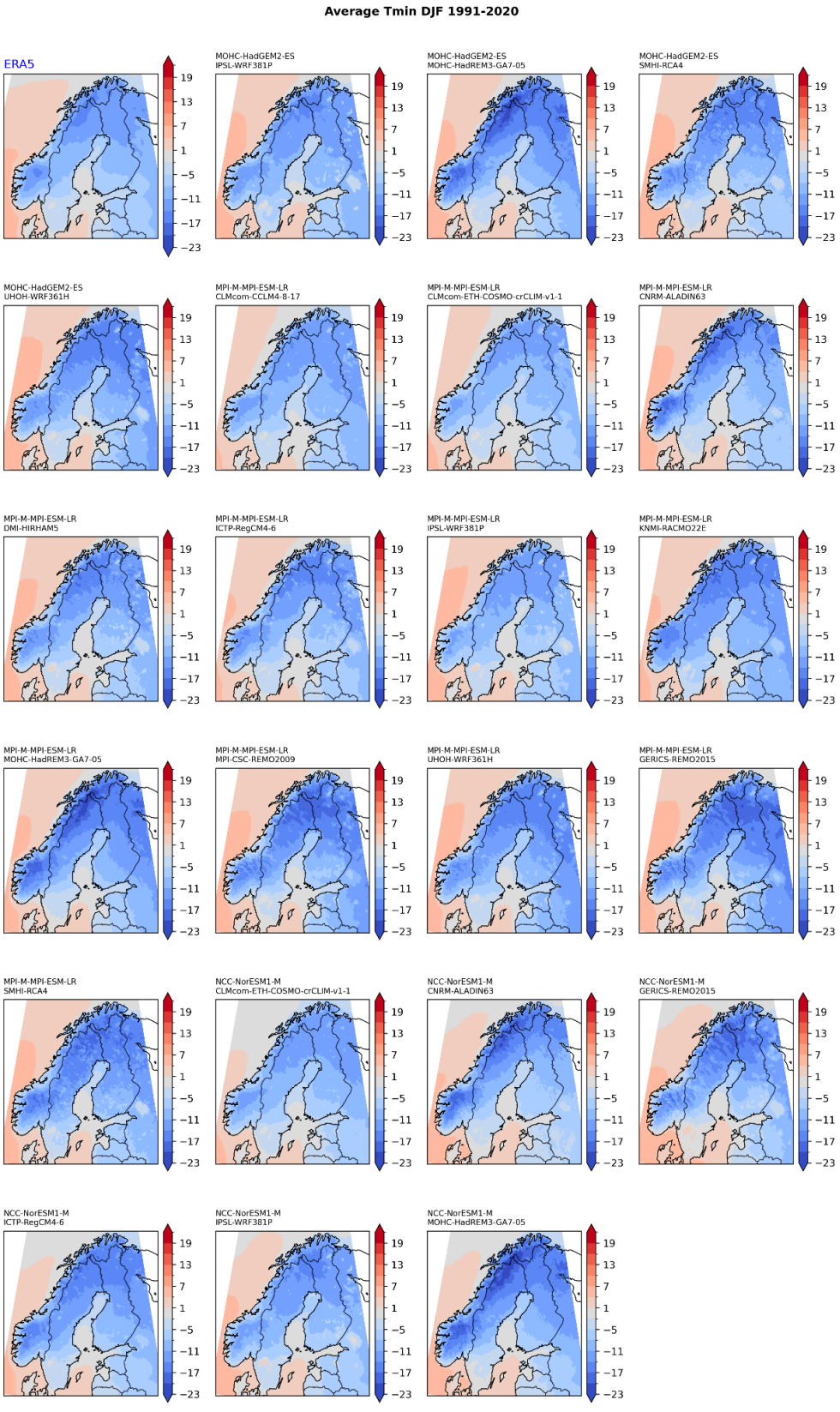

Figure A5. Cont

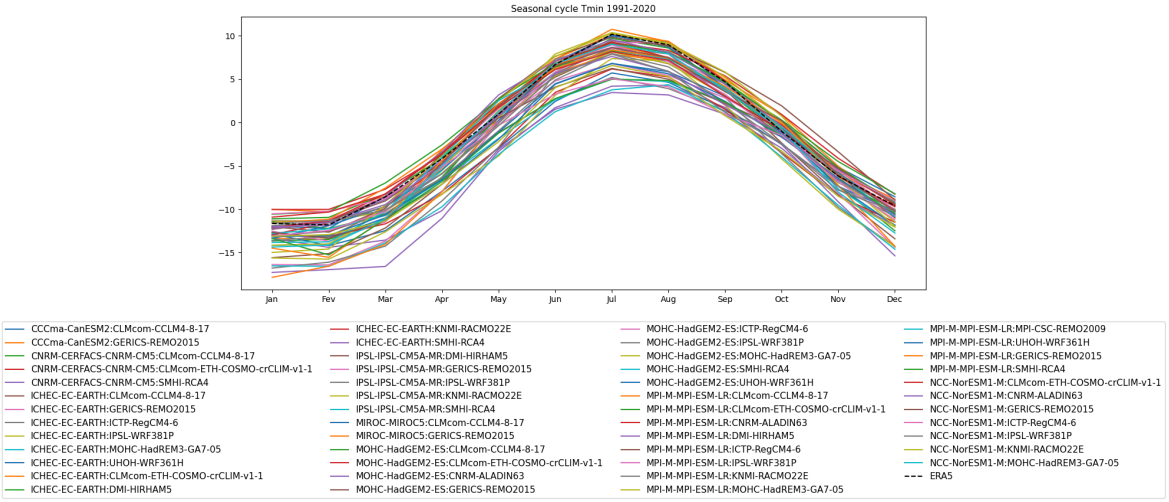

Figure A6. Same as A3 but for CORDEX.

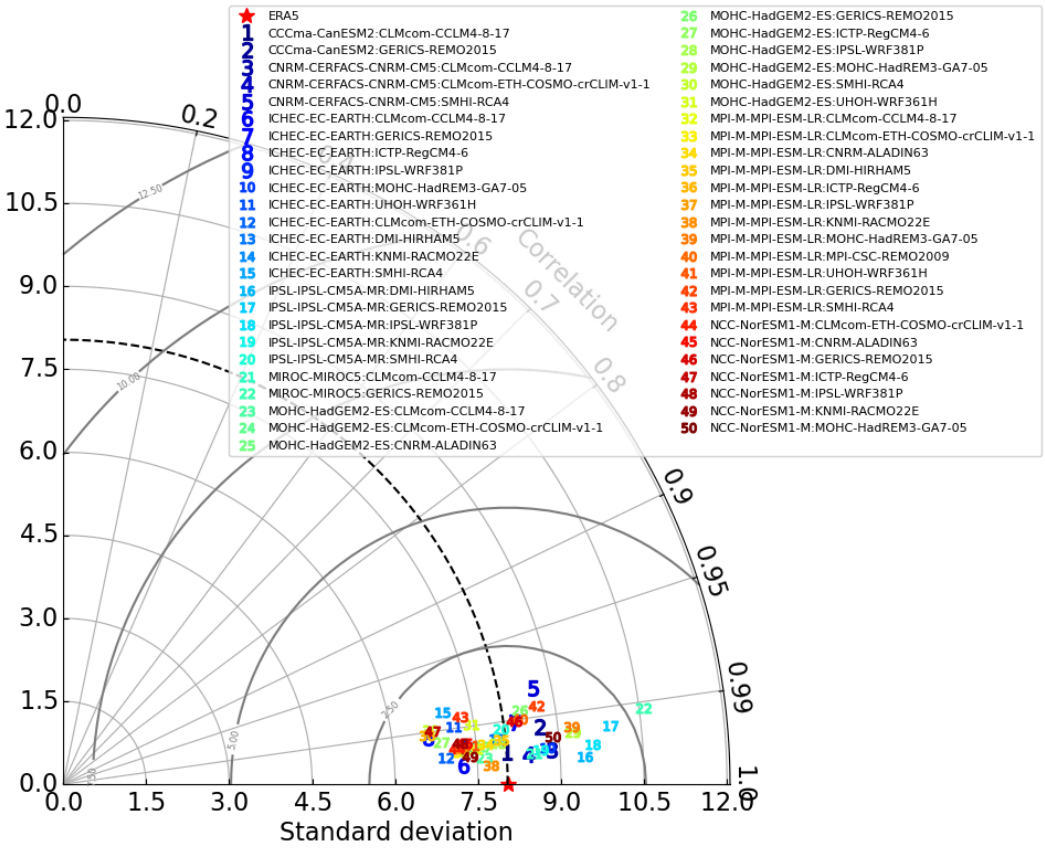

Figure A7. Same as A4 but for CORDEX

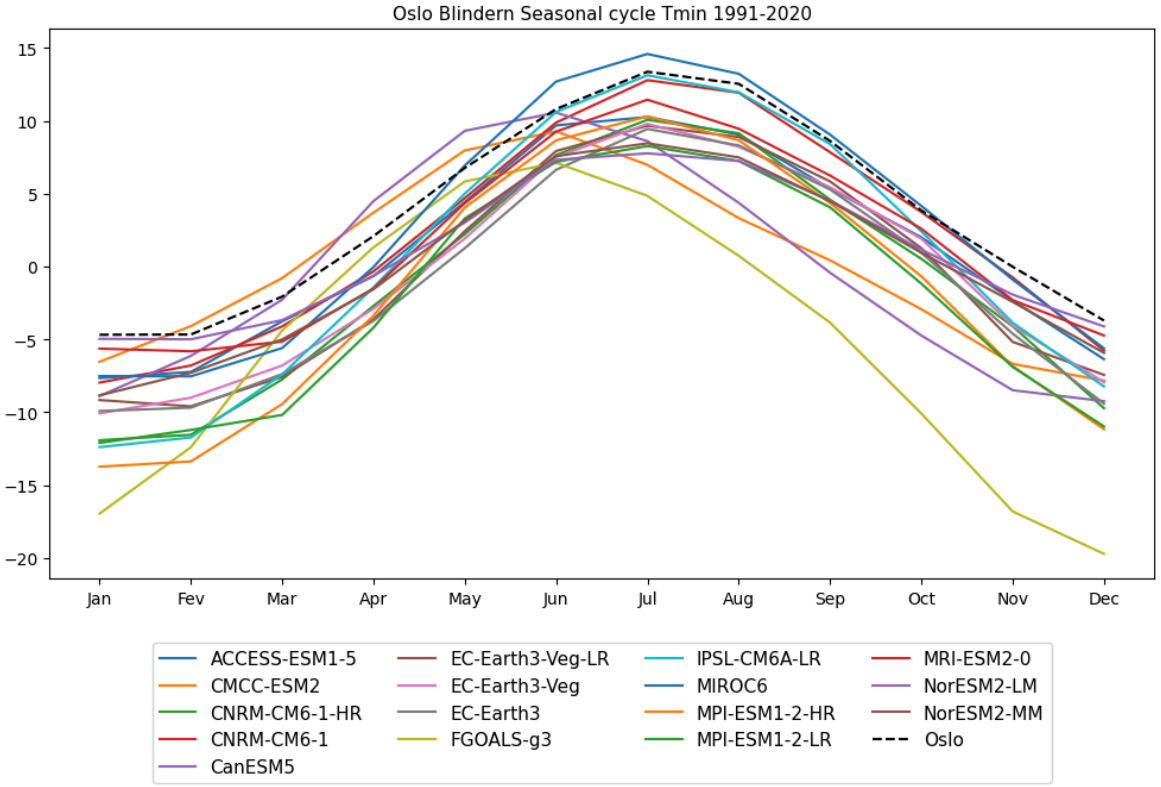

Figure A8 Same as A3 but for Oslo

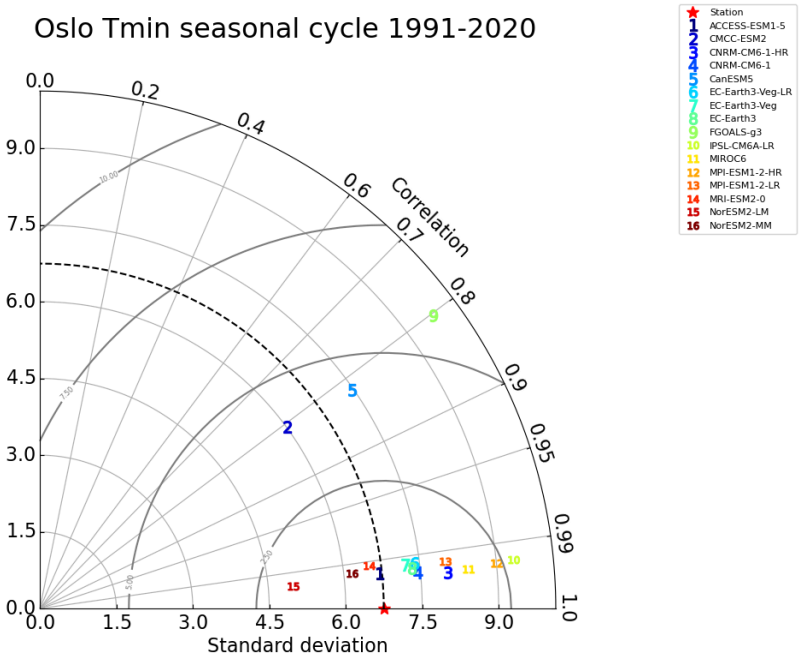

Figure A9 Same as A4 but for Oslo

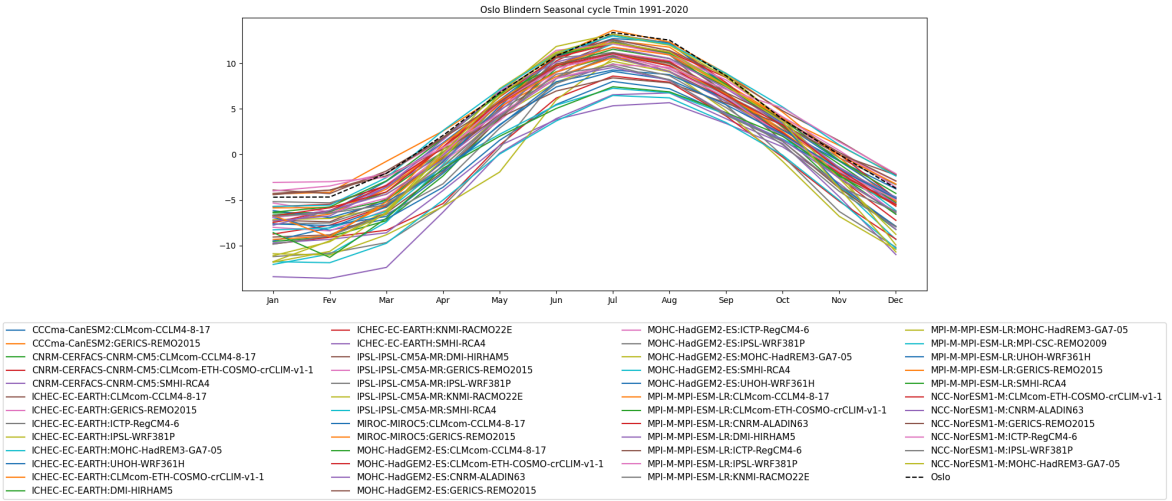

Figure A10. Same as A6 but for Oslo.

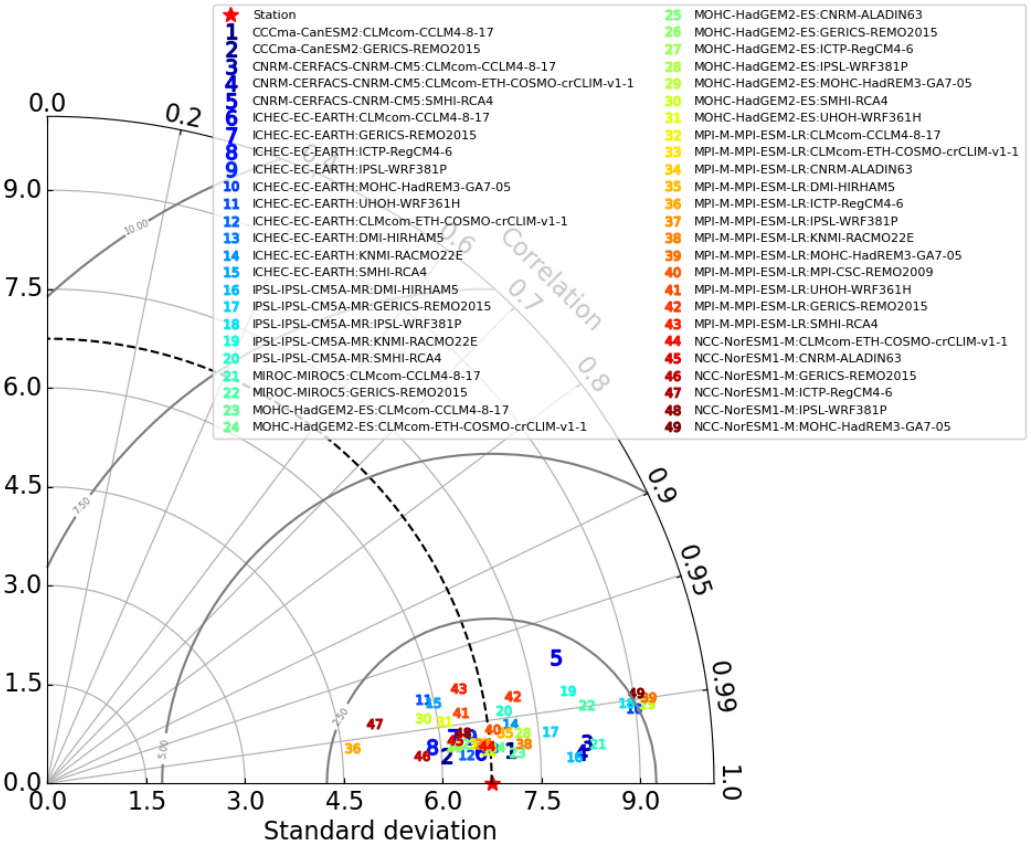

Figure A11. Same as A7 but for Oslo